Journal of Medicinal Chemistry

Featured Article

pubs.acs.org/jmc

Synthesis and Biological Evaluation of the 1-Arylpyrazole Class of σ_1 Receptor Antagonists: Identification of 4-{2-[5-Methyl-1-(naphthalen-2-yl)-1*H*-pyrazol-3-yloxy]ethyl}morpholine (S1RA, E-52862)

José Luis Díaz,*[,†] Rosa Cuberes,[†] Joana Berrocal,[†] Montserrat Contijoch,[†] Ute Christmann,[†] Ariadna Fernández,[†] Adriana Port,[†] Jörg Holenz,[†] Helmut Buschmann,[†] Christian Laggner,[‡] Maria Teresa Serafini,[†] Javier Burgueño,[†] Daniel Zamanillo,[†] Manuel Merlos,[†] José Miguel Vela,[†] and Carmen Almansa[†]

[†]Drug Discovery and Preclinical Development, Esteve, Av. Mare de Déu de Montserrat, 221, 08041, Barcelona, Spain

[‡]Department of Drug and Natural Product Synthesis, Faculty of Life Sciences, University of Vienna, Althanstrasse 14, A-1090 Vienna, Austria

Supporting Information

ABSTRACT: The synthesis and pharmacological activity of a new series of 1-arylpyrazoles as potent σ_1 receptor (σ_1R) antagonists are reported. The new compounds were evaluated in vitro in human σ_1R and guinea pig σ_2 receptor (σ_2R) binding assays. The nature of the pyrazole substituents was crucial for activity, and a basic amine was shown to be necessary, in accordance with known receptor pharmacophores. A wide variety of amines and spacer lengths between the amino and pyrazole groups were tolerated, but only the ethylenoxy spacer and small cyclic amines provided compounds with sufficient selectivity for σ_1R vs σ_2R. The most selective compounds were further profiled, and compound **28**, 4-{2-[5-methyl-1-(naphthalen-2-yl)-1*H*-pyrazol-3-yloxy]ethyl}morpholine (S1RA, E-52862), which showed high activity in the mouse capsaicin model of neurogenic pain, emerged as the most interesting candidate. In addition, compound **28** exerted dose-dependent antinociceptive effects in several neuropathic pain models. This, together with its good physicochemical, safety, and ADME properties, led compound **28** to be selected as clinical candidate.

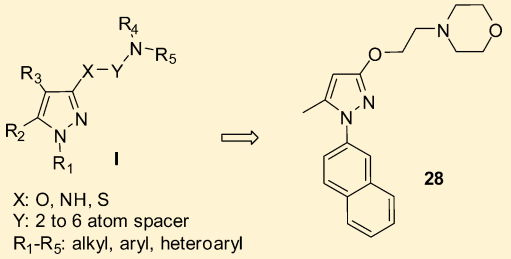

INTRODUCTION

The σ receptors were discovered 35 years ago and later on classified as σ_1 and σ_2, based on their size, tissue distribution, and drug selectivity patterns.[1] σ_1R has been cloned and shown to encode a protein of 223 amino acids anchored to the endoplasmic reticulum and plasma membranes.[2] This protein acts as a unique ligand-regulated molecular chaperone[3] that modulates the activity of different proteins, such as *N*-methyl-D-aspartic (NMDA) receptors[4] and several ion channels.[5] Additionally, since the early 1990s σ_1R has been known to modulate opioid analgesia,[6] and the relationship between the μ-opioid and σ_1R has been recently shown to involve direct physical interaction,[7] which explains why σ_1R antagonists enhance the antinociceptive effect of opioids.

Research has been done on the therapeutic potential of σ_1R ligands. While several compounds have undergone clinical studies as antidepressants, drug abuse treatments, antipsychotics, and agents for improvement in learning and memory, no selective σ_1R ligands have so far been marketed.[8] Several compounds have been extensively used as pharmacological tools: (+)-pentazocine (**1**) and PRE-084 (**2**) as σ_1R agonists.[6] Conversely, BD-1063 (**3**) and haloperidol (**4**), which also antagonize dopamine receptors, are typical σ_1R antagonists[9] (Figure 1). On the other hand, σ_2R has recently been shown to be involved in cellular proliferation and cell death. Indeed, agonists acting on this receptor show proapoptotic properties, thus suggesting a potential role in cancer treatment.[10] Because the two

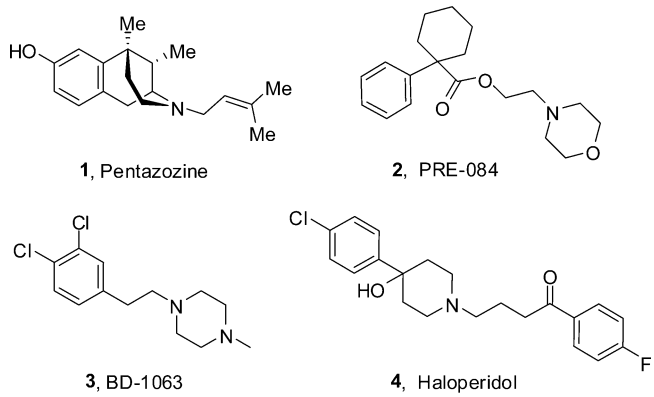

Figure 1. Representative σ_1R agonists (**1**, **2**) and antagonists (**3**, **4**).

Received: May 25, 2012
Published: July 12, 2012

dx.doi.org/10.1021/jm3007323 | *J. Med. Chem.* 2012, 55, 8211−8224

Scheme 1[a]

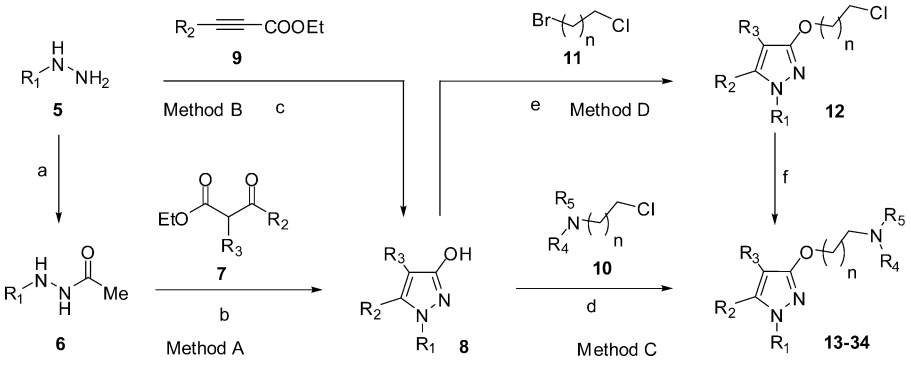

[a]Reagents and conditions: (a) Ac_2O, toluene, rt; (b) PCl_3, 50 °C; (c) *t*-BuOK, *t*-BuOH, rt; (d) K_2CO_3, NaI, DMF, 70 °C or NaH, DMF, 60 °C; (e) K_2CO_3, NaI, DMF, rt; (f) NHR_4R_5, K_2CO_3, NaI, DMF, toluene, reflux.

Table 1. 3-Aminoethoxy-1-(3,4-dichlorophenyl)pyrazoles

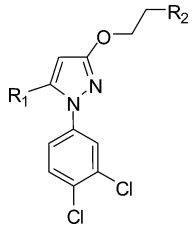

compd	R_1	R_2	$K_i\sigma_1$[a] (*h*, nM)	$K_i\sigma_2$[b] (*gp*, nM)	M[c]
3			6.3 ± 1.7	318.4 ± 62.3	
4			2.1 ± 0.3	22.0 ± 1.4	
13a	Me	Morpholin-4-yl	10.8 ± 1.8	> 1000	A, C
13b	Me	Pyrrolidin-1-yl	5.2 ± 2.3	483 ±161	A, C
13c	Me	Piperidin-1-yl	5.5 ± 1.2	209 ± 40	A, C
13d	Me	Homopiperidin-1-yl	9.4 ± 0.3	63.5 ± 53.5	A, D
13e	Me	4-Methylpiperidin-1-yl	8.4 ± 1.0	161 ± 36	A, D
13f	Me	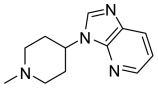	16.0 ± 1.2	435 ± 232	A, D
13g	Me	4-Methylpiperazin-1-yl	11.1 ± 0.5	> 1000	A, D
13h	Me	1-Ethoxycarbonylpiperazin-4-yl	44.0 ± 0.9	> 1000	A, D
13i	Me	4-Phenylpiperazin-1-yl	14.8 ± 3.7	563 ± 171	A, D
13j	Me	Diethylamino	9.9 ± 0.3	250 ± 34	A, C
13k	Me	Cyclohexylamino	8.5 ± 0.2	8.8 ± 6.7	A, D
13l	Me	Imidazol-1-yl	294 ± 29	> 1000	A, C
14a	H	Morpholin-4-yl	8.2 ± 0.7	280 ± 214	B, C
14b	H	Pyrrolidin-1-yl	15.7 ± 2.7	23.7 ± 12.8	B, C
14c	H	Piperidin-1-yl	16.7 ± 1.2	64.7 ± 19.6	B, C
14d	H	Homopiperidin-1-yl	8.9 ± 0.9	8.9 ± 13.4	B, D
14e	H	4-Methylpiperidin-1-yl	8.6 ± 1.2	32.8 ± 43.6	B, D
14f	H	4-Acetylpiperazin-1-yl	7.2 ± 1.1	> 1000	B, D
15	Pr^i	Morpholin-4-yl	172 ± 32	> 1000	A, C
16	Ph	Morpholin-4-yl	224 ± 1	> 1000	A, D

[a]Binding affinity to human σ_1R in transfected HEK-293 membranes using [^{3}H](+)-pentazocine as radioligand. Each value is the mean ± SD of two determinations. [b]Binding affinity to σ_2R in guinea pig brain membranes using [^{3}H]di-*o*-tolylguanidine as radioligand. Each value is the mean ± SD of two determinations. [c]Methods used for the synthesis of compounds according to Scheme 1.

receptors are clearly differentiated pharmacologically, selectivity between the two and versus other targets is desired.

Our group became interested in the potential role of σ_1R in pain control, and a σ_1R knockout mouse was developed. σ_1R knockout mice show attenuated pain responses in the formalin test,[11] and no mechanical hypersensitivity following capsaicin sensitization[12] or sciatic nerve injury was observed.[13] Haloperidol was also shown to inhibit formalin-induced pain and capsaicin-induced hypersensitivity.[14] Other authors identified the spinal cord as the main site of action, as both nociceptive behaviors and molecular mechanisms underlying central sensitization (i.e., phosphorylation of the NR1 subunit of the NMDA receptor in the spinal cord) were inhibited by spinal administration of a σ_1R antagonist.[15] These results, together with the key role played by σ_1R in pain-related central sensitization phenomena,[13,16] support the involvement of σ_1R in the control of nociception.

On the basis of these findings, an internal program aimed at identifying σ_1R antagonists for the treatment of pain was initiated and led to several active series.[17] In continuation of our efforts in

dx.doi.org/10.1021/jm3007323 | J. Med. Chem. 2012, 55, 8211−8224

Scheme 2[a]

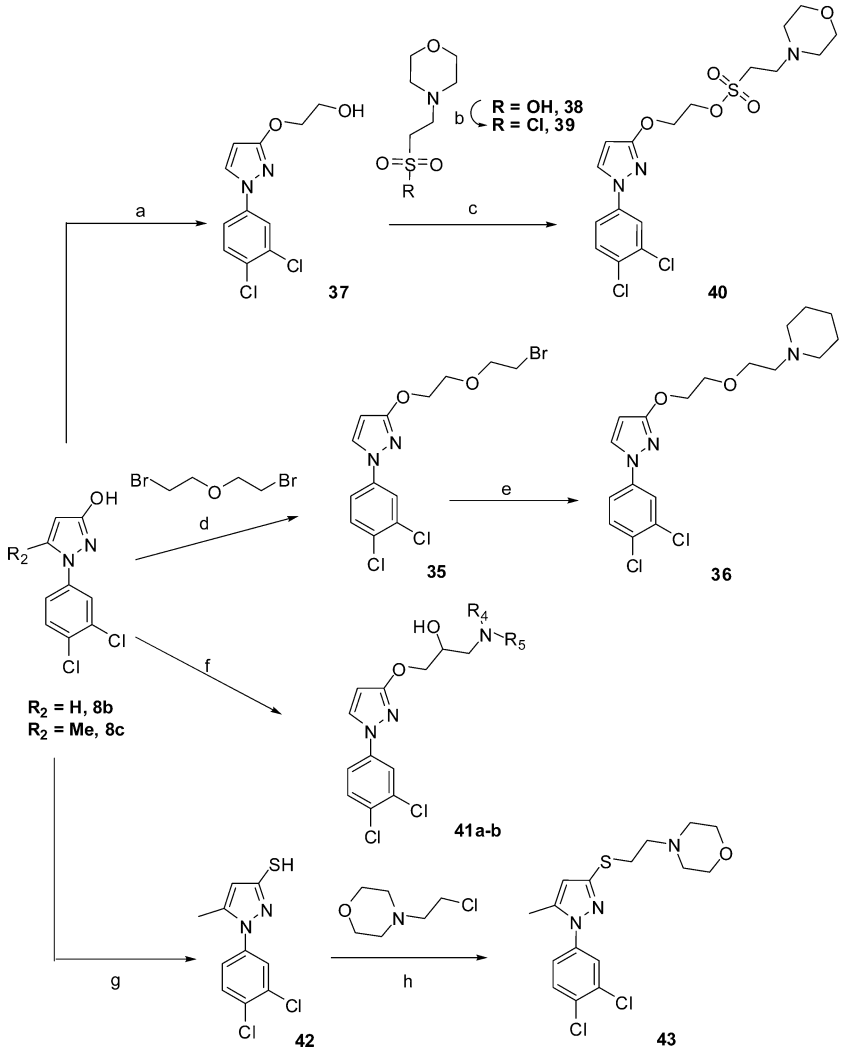

[a]Reagents and conditions: (a) 2-bromoethanol, K_2CO_3, NaI, DMF, 60 °C, 18 h; (b) oxalyl chloride, CH_2Cl_2, 0 °C; (c) triethylamine, CH_2Cl_2, rt, 18 h; (d) K_2CO_3, NaI, DMF, rt, 18 h; (e) NHR_4R_5, K_2CO_3, NaI, DMF, 100 °C, 18 h; (f) (i) 2-(chloromethyl)oxirane, K_2CO_3, NaI, DMF, 100 °C, 4 h; (ii) NHR_4R_5, K_2CO_3, NaI, DMF, 100 °C, 8 h; (g) (i) P_2S_5, xylene, reflux, 19 h; (ii) $NaBH_4$, EtOH, reflux, 16 h; (h) K_2CO_3, NaI, DMF, 95 °C, 18 h.

this field, we report herein the structure−activity relationship (SAR) studies of a series of 1-arylpyrazoles that led to the discovery of 4-{2-[5-methyl-1-(naphthalen-2-yl)-1*H*-pyrazol-3-yloxy]ethyl}morpholine (S1RA, E-52862, **28**). Compound **28** is a highly selective σ_1R antagonist[18] and has successfully completed phase I safety and pharmacokinetic evaluation in humans.[19] It is currently undergoing phase II clinical trials for the treatment of pain and is the first-in-class compound to be developed for this indication.

CHEMISTRY

The synthesis of the new compounds was accomplished using different routes, as outlined in Schemes 1−4.[20] As depicted in Scheme 1, aminoalkoxypyrazoles **13**−**34** were obtained using four alternative procedures. Depending on the substitution pattern of the final pyrazole, the key intermediate 3-hydroxypyrazole **8** was prepared through a one-step (method B) or a two-step (method A) procedure from aryl- or alkylhydrazines **5**. Method A involved acetylation with acetic anhydride to give hydrazides **6** in good yields and subsequent cyclization with ethyl 3-oxoalkanoates **7** to give **8** in moderate yields.[21] Method B afforded **8** in one step and around 50% yield on treatment of **5** with ethyl 3-functionalized propinoates **9**.[22] The high regioselectivity of both methods was shown on account of 5-hydroxypyrazole not being isolated in any case. Final compounds **13**−**34** were obtained in good yields by treatment of **8** with commercially available chloroalkylamines **10** under basic conditions (method C). Alternatively, a two-step procedure (method D) was used. In this case, reaction of **8** with 1-bromo-*ω*-chloroalkanes **11** occurred with good regioselectivity to provide chloro derivatives **12**, which upon reaction with the corresponding amines under mild basic conditions afforded the final compounds in moderate yields. In the case of amide **33f** (Table 4), NaH was required for nucleophilic substitution. General methods A−D are described in the experimental part, and the specific procedures used for the preparation of each of the derivatives **13**−**34** are indicated in Tables 1−4.

Elongated analogues **36**, **40**, and **41a,b** were obtained starting from 1-(3,4-dichlorophenyl)-1*H*-pyrazol-3-ol **8b** (Scheme 2). Alkylation of **8b** with 1-bromo-2-(bromoethoxy)ethane under basic conditions provided exclusively the monosubstituted **35**, which on treatment with piperidine afforded compound **36** in

dx.doi.org/10.1021/jm3007323 | J. Med. Chem. 2012, 55, 8211−8224

Table 2. 1-(3,4-Dichlorophenyl)pyrazoles

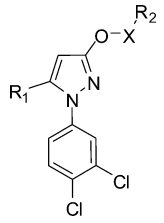

compd	R_1	X	R_2	$K_i\,\sigma_1$[a] (*h*, nM)	$K_i\,\sigma_2$[b] (*gp*, nM)	M[c]
3				6.3 ± 1.7	318.4 ± 62.3	
4				2.1 ± 0.3	22.0 ± 1.4	
17a	Me	$(CH_2)_3$	Morpholin-4-yl	18.9 ± 1.6	638 ± 467	A, D
17b	Me	$(CH_2)_3$	Pyrrolidin-1-yl	10.4 ± 1.8	62.0 ± 43.2	A, C
17c	Me	$(CH_2)_3$	4-Methylpiperazin-1-yl	13.3 ± 0.1	170 ± 59	A, D
18a	H	$(CH_2)_3$	Morpholin-4-yl	16.1 ± 3.0	394 ± 308	B, D
18b	H	$(CH_2)_3$	Piperidin-1-yl	9.6 ± 1.4	37.2 ± 6.8	B, D
18c	H	$(CH_2)_3$	4-Methylpiperazin-1-yl	16.5 ± 6.8	307 ± 131	B, D
19a	Me	$(CH_2)_4$	Morpholin-4-yl	13.3 ± 0.2	245 ± 81	A, D
19b	Me	$(CH_2)_4$	Pyrrolidin-1-yl	6.9 ± 0.1	12.6 ± 8.4	A, D
19c	Me	$(CH_2)_4$	Piperidin-1-yl	7.1 ± 0.3	47.5 ± 27.7	A, D
19d	Me	$(CH_2)_4$	4-Phenylpiperidin-1-yl	26.0 ± 3.8	26.7 ± 30.1	A, D
19e	Me	$(CH_2)_4$	4-Methylpiperazin-1-yl	9.9 ± 0.5	102 ± 22	A, D
19f	Me	$(CH_2)_4$	Diethylamino	11.7 ± 0.1	45.5 ± 21.0	A, D
19g	Me	$(CH_2)_4$	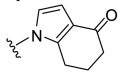	>1000	>1000	A, D
19h	Me	$(CH_2)_4$	Imidazol-1-yl	854 ± 144	>1000	A, D
20a	H	$(CH_2)_4$	Morpholin-4-yl	17.6 ± 0.1	829 ± 48	B, D
20b	H	$(CH_2)_4$	Thiomorpholin-4-yl	10.2 ± 0.5	344 ± 292	B, C
20c	H	$(CH_2)_4$	(2S,6R)-2,6-dimethylmorpholin-4-yl	14.8 ± 0.5	153 ± 60	B, D
20d	H	$(CH_2)_4$	Diethylamino	17.2 ± 6.1	104 ± 23	B, C
20e	H	$(CH_2)_4$	Benzylmethylamino	24.0 ± 0.1	46.3 ± 19.3	B, D
20f	H	$(CH_2)_4$	(2-Methoxyethyl)methylamino	8.2 ± 0.9	66.3 ± 25.8	B, C
36	H	$(CH_2)_2O(CH_2)_2$	Piperidin-1-yl	36.8 ± 0.1	14.2 ± 7.5	B
40	H	$(CH_2)_2OSO_2(CH_2)_2$	Morpholin-4-yl	879 ± 149	> 1000	B
41a	H	$CH_2CHOHCH_2$	Morpholin-4-yl	128 ± 9	> 1000	B
41b	H	$CH_2CHOHCH_2$	4-Methylpiperazin-1-yl	233 ± 52	> 1000	B

[a]Binding affinity to human σ_1R in transfected HEK-293 membranes using [^{3}H](+)-pentazocine as radioligand. Each value is the mean ± SD of two determinations. [b]Binding affinity to σ_2R in guinea pig brain membranes using [^{3}H]di-*o*-tolylguanidine as radioligand. Each value is the mean ± SD of two determinations. [c]Methods used for the synthesis of compounds according to Scheme 1.

Scheme 3[a]

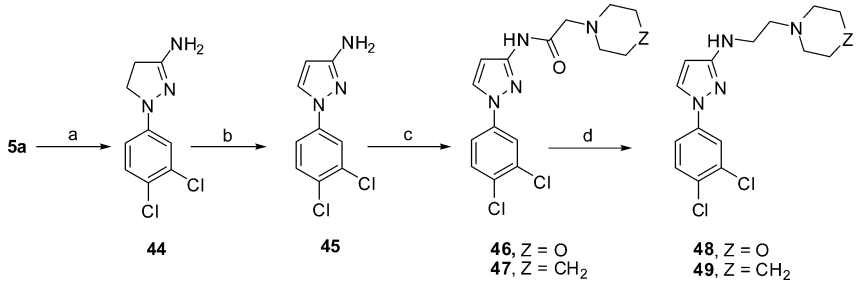

[a]Reagents and conditions: (a) NaOEt, EtOH, acrylonitrile, reflux, 24 h; (b) MnO_2, CH_2Cl_2, rt; (c) (i) triethylamine, THF, 2-chloroacetyl chloride, rt, 18 h; (ii) amine, K_2CO_3, NaI, DMF, 100 °C, 18 h; (d) 2 M BH_3·Me_2S in THF, THF, reflux, 4 h.

70% overall yield. Sulfonate ester **40** was obtained by alkylation of **8b** with 2-bromoethanol and subsequent sulfonation of the resulting **37** with sulfonyl chloride **39**, which was prepared by treatment of **38** with oxalyl chloride. Hydroxyl derivatives **41** were prepared by treatment of **8b** with 2-(chloromethyl)oxirane under basic conditions, followed by ring-opening with morpholine or piperidine, which took place over the less substituted oxirane position to afford **41a** and **41b**, respectively (Table 2).

Thiopyrazole **43** was prepared by treatment of **8c** with phosphorus pentasulfide to provide **42**, which was subsequently alkylated with chloroethylmorpholine using conditions similar to those used for hydroxy derivatives.

The route depicted in Scheme 3 was used for the preparation of aminopyrazoles **47**–**49**. 3,4-Dichlorophenylhydrazine, **5a**, was reacted with acrylonitrile[23] to provide the red pyrazoline **44**, which upon oxidation with manganese dioxide gave aminopyrazole **45**. Treatment of **45** with 2-chloroacetyl chloride and subsequent substitution with morpholine or piperidine afforded amides **46** and **47** in excellent yields. Final reduction with borane dimethylsulfide provided amines **48** and **49** in moderate yields.

dx.doi.org/10.1021/jm3007323 | *J. Med. Chem.* 2012, 55, 8211–8224

For the sake of comparison, the preparation of the 5-oxy regioisomer of the most interesting compound, **28**, was undertaken (Scheme 4). *N*-Boc protection of hydroxypyrazole

Scheme 4[a]

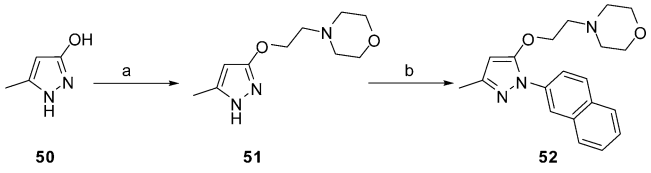

[a]Reagents and conditions: (a) (i) $(Boc)_2O$, CH_2Cl_2, triethylamine, rt, 18 h; (ii) 4-(2-chloroethyl)morpholine hydrochloride, K_2CO_3, KI, DMF, 95 °C; (iii) EtOH, 3 N HCl; (iv) NaOH; (b) 2-naphthaleneboronic acid, $Cu(OAc)_2$, pyridine, 4 Å molecular sieves, CH_2Cl_2, air, 16 h, rt.

50, followed by treatment with 4-(2-chloroethyl)morpholine and deprotection, provided compound **51**. Arylation of **51** with 2-naphthylboronic acid under Chan−Lam conditions[24] provided a 2:1 mixture of the 5- and 3-oxy regioisomers, which were separated by chromatography to give **52** in 30% yield along with 15% yield of **28**.

RESULTS AND DISCUSSION

The design of the new series was performed taking into account the known pharmacophoric features of σ_1R. As recently summarized by Wünsch et al.,[25] several pharmacophores reported in the literature share a basic amino group and at least two hydrophobic regions at a certain distance from the basic amino group. According to the model by Glennon et al.,[26] the distances are defined as 2.5−3.9 and 6−10 Å (Figure 2 A), while

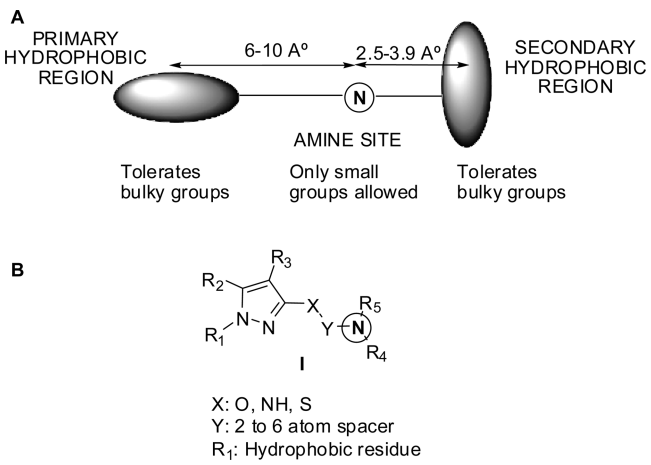

Figure 2. Pharmacophoric σ_1R model by Glennon[26] (A) and general structure of the new 1-arylpyrazoles **I** (B).

the model by Laggner et al.[27] suggests two additional hydrophobic groups. Compounds of general structure **I** (Figure 2 B) were designed in which the pyrazole ring was foreseen as a good scaffold to be decorated with different groups in order to comply with said pharmacophoric requirements as well as to explore other possibilities.

The new compounds were first evaluated in vitro by determining their binding affinities for σ_1 and σ_2 receptors using [^{3}H](+)-pentazocine[28] and [^{3}H]di-*o*-tolylguanidine,[29] respectively, as radioligands. The results of these primary assays are reported in Tables 1−5. For the sake of comparison, the results of reference compounds **3** and **4** are included in all tables.

The SAR study was initiated with the introduction, at position 1 of the pyrazole ring, of a 3,4-dichlorophenyl group which was present in known σ_1R ligands, such as **3**,[30] and using a morpholino group also common in σ_1R ligands, such as **2**. The ethylene linker was selected because the resulting seven bond length between the aromatic and the amine group could fit pharmacophoric requirements. The first compound prepared, **13a**, showed good σ_1R binding affinity and selectivity toward the σ_2R, which encouraged further exploration of the different positions. The 3,4-dichlorophenyl group at position 1 and the ethylene linker were maintained to explore the nature of the amino group (Table 1). The substitution of morpholino by carbonated cyclic analogues provided good σ_1R potency, but selectivity vs the σ_2R receptor decreased in the following order: morpholinyl (**13a**), pyrrolidinyl (**13b**), piperidinyl (**13c**), homopiperidinyl (**13d**), and 4-methylpiperidinyl (**13e**). Bulkier substituents, such as the pyridoimidazolyl group of **13f** or the phenyl group of **13i**, which probably occupy the second hydrophobic region of the receptor, were tolerated but led to decreased selectivity. The piperazine derivatives substituted with smaller groups, **13g,h**, were potent and selective, thus suggesting that small polar groups are preferred in terms of selectivity. Open chain amines, such as diethylamino **13j** and cyclohexylamino **13k**, showed good potency but low selectivity, and the introduction of an imidazole group resulted in significantly reduced potency for both receptors (**13l**), unsurprisingly so given the low basicity of the imidazole nitrogen.

Some 5-unsubstituted analogues were prepared that were shown to have similar σ_1R binding affinity but diminished selectivity compared to their methylated counterparts (see **14a−e** vs **13a−e**, respectively). Conversely, the 4-acetylpiperazinyl derivative **14f** showed excellent selectivity, again suggesting that this more polar group was not tolerated by the σ_2R binding site. Position 5 was further explored by introducing bulkier groups, such as *i*-Pr (**15**) and phenyl (**16**), which resulted in great loss of potency.

The effect of increasing the distance between the pyrazole ring and the basic nitrogen atom was then explored. As shown in Table 2, propylene derivatives **17a−c** maintained σ_1R potency, but affinity for σ_2R increased vs their ethylene counterparts (**13a,b,h**, respectively). In this case, the 5-unsubstituted derivatives **18a−c** were quite similar to their methylated analogues in terms of potency and selectivity. Further elongation of the spacer provided derivatives **19** and **20**, which showed similar or increased σ_2R affinity vs their propylene counterparts. The introduction of an additional aromatic group to reach the second hydrophobic region provided potent compounds **19d** and **20e**, which again were equipotent for σ_2R. Selectivity was not improved by morpholino replacement with thiomorpholino (**20b**) or by methylation of the morpholine ring (**20c**) or by introduction of oxygen atoms in the alkyl chains (**20f**). As shown with the ethylene spacer, the reduced basicity of the nitrogen atoms was clearly detrimental for activity (**19g,h**). A five-atom spacer with an intercalated oxygen atom (**36**) maintained potency for both receptors, while the six-atom sulfonate ester spacer, **40**, was not tolerated. The introduction of a hydroxyl group in the linker provided a decrease in the potency of both receptors (**41a,b** vs **18a,c**), thus suggesting that polar groups are not preferred in this region.

The morpholinoethoxy group emerged as one of the best moieties in terms of selectivity and was thus selected for further

dx.doi.org/10.1021/jm3007323 | J. Med. Chem. 2012, 55, 8211−8224

Table 3. Morpholinoethyloxypyrazoles

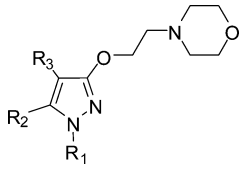

compd	R_1	R_2	R_3	$K_i\ \sigma_1$ [a] (h, nM)	$K_i\ \sigma_2$ [b] (gp, nM)	M[c]
3				6.3 ± 1.7	318.4 ± 62.3	
4				2.1 ± 0.3	22.0 ± 1.4	
21	3,4-dichlorophenyl	Me	Me	9.4 ± 1.8	351 ± 400	A, D
22	3,4-dichlorophenyl	Me	COMe	741 ± 134	>1000	A, C
23	phenyl	Me	H	>1000	>1000	A, C
24	4-methoxyphenyl	Me	H	>1000	>1000	A, C
25	3-chlorophenyl	Me	H	180 ± 28	>1000	A, C
26	4-chlorophenyl	H	H	17.8 ± 1.5	357 ± 357	B, C
27	2,4-dichlorophenyl	Me	H	44.0 ± 11.0	>1000	A, C
28	2-naphthyl	Me	H	17.0 ± 7.0[d]	>1000	A, C
29	2-naphthyl	H	H	33.3 ± 4.0	>1000	B, C
30	2-naphthyl	Me	Me	139 ± 9	>1000	A, C
31	*tert*-butyl	H	H	>1000	>1000	B, C
32	cyclohexyl	H	H	23.1 ± 3.9	>1000	B, C

[a]Binding affinity to human σ_1R in transfected HEK-293 membranes using [^{3}H](+)-pentazocine as radioligand. Each value is the mean ± SD of two determinations. [b]Binding affinity to σ_2R in guinea pig brain membranes using [^{3}H]di-*o*-tolylguanidine as radioligand. Each value is the mean ± SD of two determinations. [c]Methods used for the synthesis of compounds according to Scheme 1. [d]See ref 18.

Table 4. 1-Naphthalen-2-ylpyrazoles

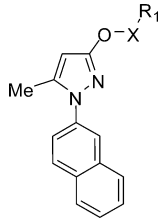

compd	X	R_1	$K_i\ \sigma_1$ [a] (h, nM)	$K_i\ \sigma_2$ [b] (gp, nM)	M[c]
3			6.3 ± 1.7	318.4 ± 62.3	
4			2.1 ± 0.3	22.0 ± 1.4	
33a	$(CH_2)_2$	piperidin-1-yl	10.0 ± 0.7	84.7 ± 1.1	A, C
33b	$(CH_2)_2$	pyrrolidin-1-yl	9.9 ± 0.4	395 ± 96	A, C
33c	$(CH_2)_2$	diethylamino	47.0 ± 1.4	589 ± 65	A, C
33d	$(CH_2)_2$	(2*S*,6*R*)-2,6-dimethylmorpholin-4-yl	33.8 ± 4.8	>1000	A, D
33e	$(CH_2)_2$	4-acetylpiperazin-1-yl	83.4 ± 3.7	>1000	A, D
33f	$(CH_2)_2$	3-oxomorpholin-4-yl	>1000	>1000	other[d]
34a	$(CH_2)_4$	morpholin-4-yl	99.1 ± 19.5	428 ± 122	A, D
34b	$(CH_2)_4$	(2*S*,6*R*)-2,6-dimethylmorpholin-4-yl	65.0 ± 21.2	226 ± 26	A, D
34c	$(CH_2)_4$	4-acetylpiperazin-1-yl	296 ± 15	324 ± 69	A, D

[a]Binding affinity to human σ_1R in transfected HEK-293 membranes using [^{3}H](+)-pentazocine as radioligand. Each value is the mean ± SD of two determinations. [b]Binding affinity to σ_2R in guinea pig brain membranes using [^{3}H]di-*o*-tolylguanidine as radioligand. Each value is the mean ± SD of two determinations. [c]Methods used for the synthesis of compounds according to Scheme 1. [d]See experimental part for the synthesis of **33f**.

exploration of the SAR around **I** (Table 3). Substitution at position 4 of the pyrazole ring provided dimethyl derivative **21**, which maintained σ_1R potency but lost selectivity as compared to **13a**, and 4-acetyl derivative **22**, which in turn lost potency for both receptors. The nature of the group at position 1 was key for activity. Indeed, phenyl (**23**) and methoxyphenyl (**24**) were devoid of activity, while 3-chlorophenyl (**25**) led to substantially decreased potency. In contrast, the 4-chlorophenyl (**26**), 2,4-dichlorophenyl (**27**), and naphthyl (**28**, **29**) derivatives showed good affinity for σ_1R and selectivity against σ_2R. In the naphthyl series, methylation at position 4 was again shown to be detrimental for activity (**30**). Replacing the aromatic group at position 1 with *tert*-butyl (**31**) provided a complete loss of potency, while the cyclohexyl group (**32**) maintained potency and selectivity, thus suggesting the need for a ring in this position. Naphthyl **29** and cyclohexyl **32** were the only 5-unsusbtituted derivatives that showed comparatively good selectivities for σ_1R vs their methylated counterparts.

After identification of the 2-naphthyl group as an interesting substituent at position 1, both in terms of potency and selectivity, several analogues were prepared where the methyl group at position 5 was also fixed. As described in Table 4, the 1-

dx.doi.org/10.1021/jm3007323 | *J. Med. Chem.* 2012, 55, 8211−8224

pyrrolidinyl (**33b**), 2,6-dimethyl-4-morpholinyl (**33d**), and 4-acetylpiperazinyl (**33e**) derivatives were rather selective, but this good selectivity was lost on elongation to the butylene spacer (**34a−c**). Several unsubstituted analogues at position 5 were also prepared in the naphthyl series but failed to show any substantial improvement vs their methylated counterparts (results not shown).

Finally, the replacement of the oxygen atom adjacent to the pyrazole ring by NH or S (Table 5) showed that the thio (**43**)

Table 5. Amino and Thiopyrazoles

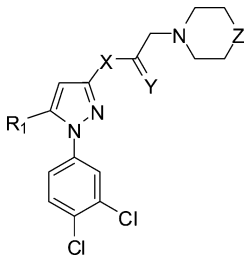

compd	R_1	X	Y	Z	$K_i\ \sigma_1$ [a] (h, nM)	$K_i\ \sigma_2$ [b] (gp, nM)
3					6.3 ± 1.7	318.4 ± 62.3
4					2.1 ± 0.3	22.0 ± 1.4
43	Me	S	H_2	O	14.2 ± 4.4	>1000
47	H	NH	O	CH_2	80.8 ± 30.2	>1000
48	H	NH	H_2	O	39.4 ± 6.4	562 ± 60
49	H	NH	H_2	CH_2	9.5 ± 4.7	90.5 ± 42.8

[a]Binding affinity to human σ_1R in transfected HEK-293 membranes using [^{3}H](+)-pentazocine as radioligand. Each value is the mean ± SD of two determinations. [b]Binding affinity to σ_2R in guinea pig brain membranes using [^{3}H]di-*o*-tolylguanidine as radioligand. Each value is the mean ± SD of two determinations.

and amino derivatives (**48**, **49**) bound both σ_1R and σ_2R in a way similar to their oxygenated analogues **13a**, **14a**, and **14c**, respectively. The amide **47** showed better selectivity but somewhat diminished potency.

The SAR summarized in Tables 1−5 shows that the nature of the pyrazole substituents is crucial for the potency of both σ_1R and σ_2R. Only certain substituted aromatics and cyclohexyl groups were tolerated at position 1. Substitution at position 4 was clearly detrimental, and only small substituents (H and methyl) were tolerated at position 5. There was also a clear need for a basic amine, as substantiated by the poor potency of derivatives **13l** and **19g,h**, which was further confirmed by the inactivity of compound **33f** (Table 4), the amide analogue of **28**. Compound **52**, a regioisomer of **28**, was also devoid of activity (K_i of σ_1, σ_2, >1000 nM), thus suggesting that requirements for achieving σ_1R activity are not as straightforward as they seem to be, based on the relatively simple pharmacophore. Regarding the amine nature, a wide variety of amines was tolerated and, interestingly, potency was not improved by adding aromatic groups (**13f**, **13i**, **19d**, **20e**) likely to reach the second hydrophobic pocket described in known σ_1R pharmacophores. Finally, spacer lengths of three to six atoms between the amine and the pyrazole groups were tolerated, although their substitution with polar groups such as hydroxyl was detrimental for activity.

Much more exquisite were the requirements for achieving good selectivity for σ_1R vs σ_2R. As mentioned above, good selectivity is desirable based on the clear-cut distinctive pharmacological functions attributed to both receptors. Generally speaking, the presence of a methyl group at position 5 increased selectivity vs unsubstituted derivatives. However, the spacer length and the nature of the amine were most crucial. As indicated in Figure 3A, where the general structure of

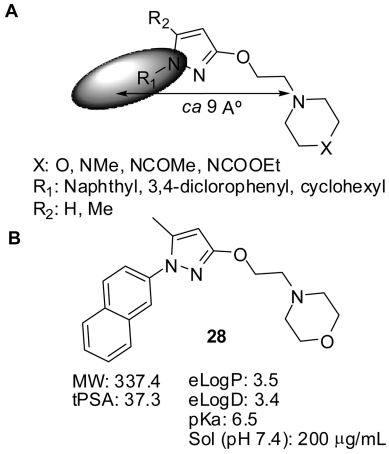

Figure 3. (A) General structure of compounds with IC_{50} < 50 nM for the σ_1R and IC_{50} > 1000 nM for the σ_2R (Table 6). (B) Structure and physicochemical properties (obtained as described in the Experimental Section) of compound **28**.

compounds with σ_1R IC_{50} < 50 nM and σ_2R IC_{50} > 1000 nM is shown, only the ethyleneoxy spacer and cyclic amines with small polar groups (morpholine and piperazines) fulfilled these criteria (see Figure 3A). σ_2R thus requires more hydrophobicity in this region, and binding affinity is favored by spacer elongation, as suggested by the increased potency of the compounds shown in Table 2.

The compounds that fulfilled the above-mentioned selectivity criteria were further profiled (Table 6). The in vitro metabolic stability in human liver microsomes[31] was evaluated and a cutoff value of intrinsic clearance (Cl_{int}) < 7 (μL/min)/mg protein was established to meet the desired profile of once-daily oral administration. Compounds were also tested in the human ether-a-go-go-related gene (hERG)[32] patch clamp assay, a well-known predictor of cardiac toxicity. In this case, a cutoff value of

Table 6. Additional Data for Compounds Complying with $K_i(\sigma_1)$ < 50 nM and $K_i(\sigma_2)$ > 1000 nM

compd	hERG[a] IC_{50} (μM)	HLM[b] Cl_{int} ((μL/min)/mg protein)	capsaicin[c] (% inhibtion at 16 mg/kg)
13a	3.5	12	25 ± 3
13g	7.4	3	27 ± 8
13h	4.1	26	NT[d]
14f	4.5	7	73 ± 6
27	>10	25	NT[d]
28[e]	>10	3	43 ± 7 62[f] ± 7
29	>10	6	55[f] ± 7
32	>10	0	20 ± 6
33d	7.4	25	NT[d]
43	>10	37	NT[d]

[a]Whole-cell patch clamp hERG blockade. [b]Intrinsic clearance in human liver microsomes as a measure of metabolic stability. [c]% reduction of mechanical hypersensitivity after ip administration of test compounds at 16 mg/kg in the mouse capsaicin test. [d]NT: not tested. [e]Capsaicin and hERG data were previously reported in ref 18. [f]Dose: 32 mg/kg.

dx.doi.org/10.1021/jm3007323 | J. Med. Chem. 2012, 55, 8211−8224

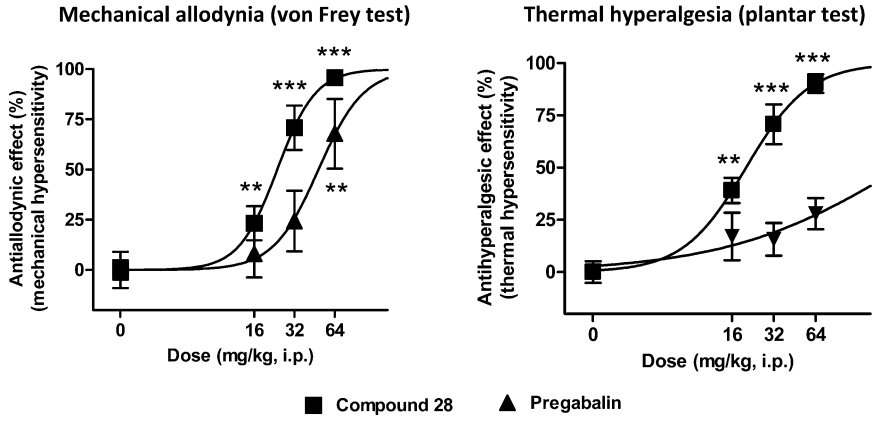

Figure 4. Dose−response effect of **28** and pregabalin on mechanical allodynia (von Frey test) and thermal (heat) hyperalgesia (plantar test) in the partial sciatic nerve ligation model of neuropathic pain. Treatments were administered by the ip route 30 (von Frey test) and 45 (plantar test) min before behavioral testing. Data were obtained from 10−12 mice per group and expressed as the mean ± SEM percentage of antiallodynic or antihyperalgesic effect: (**) $p < 0.01$, (***) $p < 0.001$ vs vehicle (dose 0) (Bonferroni's multiple comparison test after one-way ANOVA).

IC_{50} > 10 μM was established. Finally, the compounds were evaluated in vivo in a mouse model of neurogenic pain induced by intraplantar injection of capsaicin,[12] where immediate paw licking and delayed mechanical hypersensitivity are indicators of ongoing pain and pain sensitization, respectively. The inhibition of mechanical hypersensitivity was evaluated after ip administration of test compounds at 16 mg/kg.

As shown in Table 6, half of the 10 most selective compounds showed sufficient metabolic stability. Regarding hERG, five compounds showed IC_{50} inhibition higher than 10 μM and, interestingly, all contained a morpholinoethoxy group. Compounds displaying a dimethylmorpholino or a piperazino group, irrespective of the substituent type, were below the cutoff values. Regarding in vivo analgesia, several amines showed good potencies and 2-naphthyl proved to be the best group at position 1, given that **28** was superior to the 3,4-dichlorophenyl (**13a**) and cyclohexyl (**32**) derivatives. Interestingly, the two best compounds, **28** and **29**, only differed in the nature of the substituent at position 5 (Me and H, respectively). Compound **28** was somewhat superior to **29** in all tests and was thus selected for further evaluation.

The functional activity of compound **28** was evaluated using phenytoin,[33] a low potency allosteric modulator of σ_1R that shifts known σ_1R agonists to significantly higher affinities (K_i ratios without phenytoin vs with phenytoin of >1), while σ_1R antagonists show small or no shift to lower affinity values (K_i ratios without phenytoin vs with phenytoin of ≤1). Compound **28** was shown to be a σ_1R antagonist[18] on account of a small shift to lower affinity being observed when incubated in the presence of phenytoin (K_i(without phenytoin)/K_i(with phenytoin) = 0.8). Additionally, **28** was confirmed to be a highly selective compound: in addition to its low affinity for the σ_2R (K_i > 1000 nM for guinea pig and 9300 nM for rat σ_2R), it failed to show significant affinity (inhibition % at 1 μM of <50%) for another 170 molecular targets (receptors, transporters, ion channels, and enzymes).[18] The only exception to this was the human serotonin 5-HT_{2B} receptor, to which it showed moderate binding affinity (K_i = 328 nM) but very weak antagonistic activity (IC_{50} = 4700 nM).

Further in vivo evaluation of **28** was done by completing its profile in the mouse capsaicin and formalin tests. It exerted a clear dose-dependent analgesic effect on capsaicin-induced mechanical hypersensitivity and on both phases of formalin-induced pain. Its pharmacological activity was shown to correlate closely with drug levels in the brain and with actual occupancy of brain σ_1Rs.[18] Additionally, **28** potentiated morphine analgesia but not its rewarding effects[34] and showed moderate to high activity in a battery of different pain models, including carrageenan- and CFA-induced inflammatory pain and TNBS-induced chronic visceral pain models.[35]

Compound **28** was evaluated in a representative model of neuropathic pain, the partial sciatic nerve ligation model in mice,[36] and was shown to dose-dependently inhibit both mechanical allodynia and thermal hypersensitivity, with ED_{50} of 23.4 ± 0.9 and 18.8 ± 1.2 mg/kg, respectively. Interestingly, **28** showed increased potency compared to pregabalin, the gold standard for neuropathic pain treatment in humans (Figure 4). In order to discard that the observed efficacy could be due to interference with motor coordination, compound **28** was tested in the rotarod test (Figure 5), and no effect at analgesic doses was found. In contrast, analgesic doses of pregabalin induced marked motor impairment.

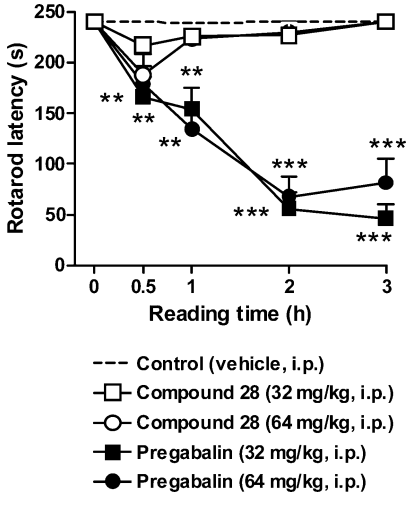

Figure 5. Dose−response effect of **28** and pregabalin on motor coordination (rotarod test). Data were obtained from 7−10 mice per group and expressed as the mean ± SEM latency (seconds) to fall-down from the rod: (**) $p < 0.01$, (***) $p < 0.001$ vs. vehicle (Bonferroni's multiple comparison test after one-way ANOVA).

dx.doi.org/10.1021/jm3007323 | J. Med. Chem. 2012, 55, 8211−8224

As shown in Figure 3, compound **28** complied with Lipinski's rules and was not highly basic, this being a desirable parameter as recently pointed out by Wager et al.[37] These authors have developed the central nervous system multiparameter optimization (CNS MPO) algorithm as a holistic approach for the prediction of good ADME and safety attributes in the case of CNS-directed compounds. An MPO value of 5.0 was calculated for **28**, which is considered to be in the high desirability range. Additionally, it also showed good permeability in Caco-2 cells[38] (370 nm/s) and an efflux ratio of 0.9, thus suggesting that it is not a substrate of efflux transporters such as glycoprotein P. All these results, together with the compound's acceptable solubility and high metabolic stability in liver microsomes, suggest good oral bioavailability in humans. Additionally, its pharmacokinetic profile was characterized in the mouse, the species used in the efficacy models. After oral administration of 10 mg/kg, compound **28** achieved a peak concentration of 622 ng/mL at 0.5 h postdosing and an AUC (area under the plasma concentration−time curve) of 958 ng·h/mL.

Finally, its potential for drug−drug interactions based on the inhibition of cytochrome P450 was evaluated in recombinant human cytochrome P450 (rhCYP) isoforms (1A2, 2B6, 2C8, 2C9, 2C19, 2D6, 2E1, and 3A4) and further studied in human liver microsomes.[39] IC_{50} values were above 10 μM in all cases, thus suggesting a low potential of compound **28** for these interactions.

In view of its interesting pharmacological, physicochemical, and ADME profile, compound **28** was selected as a preclinical candidate. Then, upon successful completion of the preclinical regulatory toxicological and pharmacodynamic package, it was selected as a clinical candidate. The ongoing clinical trials will hopefully help establish the usefulness of σ_1R antagonism as a new approach for the treatment of pain in humans, a field with strong need for new therapies.

In summary, the synthesis and pharmacological activity of a new series of 1-arylpyrazoles as potent and selective σ_1R ligands are reported here. Several compounds showed high in vitro potency as well as good antinociceptive properties, thus suggesting that σ_1R antagonization may be a useful strategy for treating pain. The most promising compound in the preclinical tests, **28**, has recently completed single and multiple dose phase I clinical studies. Upon treatment of over 250 male and female human subjects, compound **28** has shown good safety and tolerability, as well as a pharmacokinetic profile compatible with a good absorption and once-daily oral administration.[19] Proof of concept phase II studies for the treatment of neuropathic pain of different etiologies and potentiation of opioid analgesia are currently ongoing, and results will be reported in due course.

EXPERIMENTAL SECTION

Melting points were determined in open capillary tubes on a Büchi B-540 melting point apparatus and are uncorrected. ^{1}H spectra were recorded on a Varian UNITY 300 MHz (spectrometer fitted with a 5 mm H/F/X ATB probe) or a Varian Mercury 400 MHz (spectrometer fitted with a 5 mm ID/PFG probe) with 2 H lock in deuterated solvents. Chemical shifts (δ) are in parts per million. Analytical HPLC−MS was performed on a Waters 2795-MS ZQ system using reverse phase XBridge C18 columns (4.6 mm × 50 mm, 2.5 μm), gradient 2−95% B (A = 10 mM ammonium bicarbonate, B = acetonitrile) over 5.5 min, injection volume of 10 μL, and flow rate of 2.0 mL/min. PDA spectra were recorded at 220−310 nm using a Waters 2996 PDA detector. Mass spectra were obtained over the range m/z 100−800 at a sampling rate of 0.3 scans per second using Waters ZQ. Data were integrated and reported using Water Masslynx software. All compounds display purity higher than 95% as determined by this method. Accurate mass measurements were carried out using an Agilent 6540 UHD accurate-mass QTOF system and obtained by electron spray ionization (ESI) in positive mode. Elemental analyses were carried out in Institut d'Investigacions Químiques i Ambientals de Barcelona (CSIC), and results are within ±0.4% of the theoretical values. Commercially available reagents and solvents (HPLC grade) were used without further purification for all the analytical tests. Flash chromatography was performed with a forced flow of the indicated solvent system on SDS silica gel Chromagel 60 ACC (230−400 mesh).

Determination of Physicochemical Properties. Polar surface area (PSA) was calculated using ChemDraw Ultra 10.0.3. The log D, log P, and pK_a were determined by using a pH-metric technique[40] in a T3 Sirius Analytical instrument. Solubility was measured as thermodynamic solubility from solid compound in phosphate buffer at pH 7.4 by HPLC.

General Procedures for the Synthesis of 2-(1*H*-Pyrazol-3-yloxy)alkylamine Derivatives (13−34). Method A. 5-Methyl-1-(naphthalen-2-yl)-1*H*-pyrazol-3-ol (8a, R_1 = 2-naphthyl, R_2 = Me, R_3 = H). To a suspension of naphthalen-2-ylhydrazine hydrochloride (25 g, 0.128 mol) in H_2O (250 mL) was added K_2CO_3 (25 g, 0.18 mol) portionwise. After 15 min at room temperature, EtOAc (250 mL) was added and the organic layer was extracted, washed with H_2O, dried over Na_2SO_4, and concentrated to dryness. The residue was diluted in toluene (300 mL) and EtOAc (200 mL), and Ac_2O (13.1 g, 0.13 mol) was added dropwise. The solution was stirred at room temperature for 1 h, after which petroleum ether (200 mL) was added. The solution was cooled to 7 °C, and the precipitate thus formed was filtered and washed with petroleum ether to give *N*′-(naphthalen-2-yl)acetohydrazide, **6a**, as a white solid (20 g, 79%). ^{1}H NMR (DMSO-d_6) δ 9.7 (d, J = 2.6 Hz, 1 H), 7.95 (d, J = 2.6 Hz, 1 H), 7.7−7.6 (m, 3 H), 7.3 (m, 1 H), 7.15 (m, 1 H), 7.05 (dd, J = 2.3, 8.9 Hz, 1 H), 6.9 (d, J = 2.2 Hz, 1 H), 1.95 (s, 3 H).

A mixture of **6a** (20 g, 0.1 mol), ethyl 3-oxobutanoate (**7**, R_2 = Me, R_3 = H; 13.1 g, 0.1 mol), and PCl_3 (13.85 g, 0.1 mol) was heated at 50 °C for 2 h. After this time, ice was added and the solution stirred for 1 h. The suspension was poured into EtOAc and the precipitate filtered. The organic layer of the filtrate was washed, dried over Na_2SO_4, and concentrated to dryness. The residue was suspended in EtOH, filtered, and washed with cool EtOH to obtain an additional amount of 5-methyl-1-(naphthalen-2-yl)-1*H*-pyrazol-3-ol (6.47 g, 29%). ^{1}H NMR (DMSO-d_6) δ 7.95 (m, 4 H), 7.65 (dd, J = 2.3, 8.7 Hz, 1 H), 7.5 (m, 2 H), 5.65 (s, 1 H), 2.35 (s, 3 H).

Method B. 1-(3,4-Dichlorophenyl)-1*H*-pyrazol-3-ol (8b, R_1 = 3,4-dichlorophenyl, R_2 = R_3 = H). A solution of 1-(3,4-dichlorophenyl)hydrazine (7.95 g, 44.9 mmol) in *t*-BuOH (65 mL) was warmed with stirring at 30 °C, and ethyl propiolate (**9**, R_2 = H) (5.05 g, 51.5 mmol) was added dropwise. The resulting solution was cooled to 0 °C, and *t*-BuOK (11.45 g, 93.7 mmol) was added portionwise. The mixture was left to reach room temperature and stirred for 2 days. Ice was added, *t*-BuOH evaporated under vacuum, and the aqueous solution extracted with CH_2Cl_2. The remaining aqueous solution was cooled with ice, neutralized with AcOH and the resulting precipitate filtered off to afford 1-(3,4-dichlorophenyl)-1*H*-pyrazol-3-ol (**8b**; 5.3 g, 50%). ^{1}H NMR ($CDCl_3$) δ 7.65 (d, J = 2.6 Hz, 1 H), 7.6 (d, J = 2.5 Hz, 1 H), 7.5 (d, J = 8.6 Hz, 1 H), 7.35 (dd, J = 8.6 and 2.5 Hz, 1 H), 5.95 (d, J = 2.6 Hz, 1 H).

Method C. 4-{2-[5-Methyl-1-(naphthalen-2-yl)-1*H*-pyrazol-3-yloxy]ethyl}morpholine Hydrochloride (28). To a suspension of NaH (60% dispersion in mineral oil, 1.07 g, 26.8 mmol) in dry DMF (75 mL) at 0 °C was added a solution of **8a** (5.0 g, 22.3 mmol) in DMF (45 mL) dropwise. The reaction mixture was stirred at room temperature under a nitrogen atmosphere for 45 min, and then a solution of 4-(2-chloroethyl)morpholine (**10**, n = 1, NR_4R_5 = morpholine; 3.34 g, 22.3 mmol) in dry DMF (5 mL) was added. The reaction mixture was heated to 60 °C for 4 h, quenched with some drops of H_2O and the solvent removed under vacuum. The crude residue thus obtained was partitioned between diethyl ether and 2 N HCl solution. The acidic aqueous phase was washed with diethyl ether, basified by addition of 10% NaOH solution, and extracted with diethyl ether. The combined organic phases were dried over Na_2SO_4 and filtered, and the solvent was

dx.doi.org/10.1021/jm3007323 | J. Med. Chem. 2012, 55, 8211−8224

eliminated to dryness to afford 4-{2-[5-methyl-1-(naphthalen-2-yl)-pyrazol-3-yloxy]ethyl}morpholine (6.39 g, 85%) as an oil. The oil was dissolved in HCl-saturated EtOH, and the solvent was evaporated to dryness. The crude residue thus obtained was crystallized from *i*-PrOH to give the monohydrochloride as a white solid (5.24 g, 63%): mp 197−199 °C; ^{1}H NMR (DMSO-d_6) δ 10.95 (sb, 1H), 8.07−7.96 (m, 4H), 7.69 (dd, J = 8.8, 2.2 Hz, 1H), 7.63−7.52 (m, 2H), 5.92 (s, 1H), 4.57 (t, J = 4.9 Hz, 2H), 4.05−3.90 (m, 2H), 3.86−3.72 (m, 2H), 3.62−3.53 (m, 2H), 3.53−3.43 (m, 2H), 3.27−3.11 (m, 2H), 2.40 (s, 3H). Anal. ($C_{20}H_{24}ClN_3O_2$) C, H, N.

Method D. 3-(4-Chlorobutoxy)-1-(3,4-dichlorophenyl)-4,5-dimethyl-1*H*-pyrazole (12a, R_1 = 3,4-Dichlorophenyl, R_2 = R_3 = Me, *n* = 3). . A mixture of 1-(3,4-dichlorophenyl)-4,5-dimethyl-1*H*-pyrazol-3-ol (3 g, 11.7 mmol), 1-bromo-4-chlorobutane (**11**, n = 3; 6.06 g, 35 mmol), K_2CO_3 (4.83 g, 35.0 mmol), and a catalytic amount of NaI in dry DMF (25 mL) was stirred at room temperature for 18 h. The solvent was evaporated in vacuo, and the crude residue thus obtained was partitioned between H_2O and CH_2Cl_2. The organic extracts were washed with H_2O, dried over Na_2SO_4, and concentrated in vacuo to give **12a** as an oil (3.22 g, 80%): ^{1}H NMR (DMSO-d_6) δ 7.75 (d, J = 2.5 Hz, 1 H), 7.7 (d, J = 8.8 Hz, 1 H), 7.45 (dd, J = 2.5 and 8.8 Hz, 1 H), 4.2 (m, 2 H), 3.7 (m, 2 H), 2.25 (s, 3 H), 1.8 (m, 7 H).

1-(3,4-Dichlorophenyl)-4,5-dimethyl-3-[4-(pyrrolidin-1-yl)-butoxy]-1*H*-pyrazole (21). A mixture of **12a** (0.80 g, 2.3 mmol), pyrrolidine (0.19 g, 2.6 mmol), K_2CO_3 (0.95 g, 6.9 mmol), and a catalytic amount of NaI in dry DMF (20 mL) was stirred at 90 °C, under a nitrogen atmosphere, for 18 h. The solvent was evaporated in vacuo and H_2O/diethyl ether added to the residue. The organic extracts were washed with H_2O, dried over Na_2SO_4, and concentrated in vacuo to give 0.77 g of a crude product, which was purified by column chromatography (eluent, petroleum ether/EtOAc, 8/2) to afford **21** as an oil (0.43 g, 48%): ^{1}H NMR (DMSO-d_6) δ 10.85 (sb, 1 H), 7.77 (d, J = 2.4 Hz, 1 H), 7.74 (d, J = 8.8 Hz, 1 H), 7.51 (dd, J = 8.7, 2.5 Hz, 1 H), 4.59 (t, J = 4.8 Hz, 2 H), 4.04−3.91 (m, 2 H), 3.78 (t, J = 12.1 Hz, 2 H), 3.65−3.53 (m, 2 H), 3.54−3.42 (m, 2 H), 3.29−3.08 (m, 2 H), 2.28 (s, 3 H), 1.88 (s, 3 H).

4-{2-[5-Methyl-1-(naphthalen-2-yl)-1*H*-pyrazol-3-yloxy]-ethyl}morpholin-3-one (33f). To a stirred suspension of NaH (0.065 g, 60% dispersion in mineral oil, 1.63 mmol) in DMF (3 mL), cooled to 0−5 °C, was added a solution of morpholin-3-one (0.091 g, 0.91 mmol) in DMF (3 mL) dropwise. The mixture was stirred at room temperature for 3 h. After this time, a solution of 3-(2-chloroethoxy)-5-methyl-1-(naphthalen-2-yl)-1*H*-pyrazole (**12**, R_1 = 2-naphthyl, R_2 = Me, R_3 = H, n = 1; 0.20 g, 0.7 mmol) in DMF (4 mL) was added and the mixture was heated to 50 °C for 14 h. The reaction mixture was cooled, quenched with water (2 mL), and evaporated to dryness. The residue was partitioned between CH_2Cl_2 and H_2O. The organic layer was washed with water, dried over Na_2SO_4, filtered, and evaporated to give a crude residue, which was purified by column chromatography using EtOAc as eluent to afford **33f** as a white solid (0.19 g, 78%): ^{1}H NMR ($CDCl_3$) δ 7.97−7.79 (m, 4 H), 7.59 (dd, J = 8.8, 2.1 Hz, 1 H), 7.57−7.45 (m, 2 H), 5.71 (s, 1 H), 4.43 (t, J = 5.1 Hz, 2 H), 4.19 (s, 2 H), 3.87 (dd, J = 6.0, 4.2 Hz, 2 H), 3.82 (t, J = 5.1 Hz, 2 H), 3.60 (dd, J = 6.0, 4.2 Hz, 2 H), 2.37 (s, 3 H).

3-[2-(2-Bromoethoxy)ethoxy]-1-(3,4-dichlorophenyl)-1*H*-pyrazole (35). A mixture of **8b** (0.23 g, 1 mmol), 1-bromo-2-(2-bromoethoxy)ethane (0.51 g, 2 mmol), K_2CO_3 (0.42 g, 3 mmol), and NaI (0.15 g, 1 mmol) in DMF (12 mL) was stirred at room temperature under a nitrogen atmosphere for 18 h. The inorganic solid was filtered off, and the solvent was evaporated to dryness. The remaining residue was partitioned between H_2O and diethyl ether. The combined organic phases were washed with H_2O and dried over Na_2SO_4, filtered, and evaporated in vacuo. The residue was stirred with petroleum ether at 45 °C and filtered to yield, after drying, **35** which was used in the next step without further purification (466 mg): ^{1}H NMR ($CDCl_3$) δ 7.75 (d, J = 2.2 Hz, 1 H), 7.7 (d, J = 2.7 Hz, 1 H), 7.45 (m, 2 H), 5.95 (d, J = 2.7 Hz, 1 H), 4.4 (t, J = 4.4 Hz, 2 H), 4.0−3.8 (m, 4 H), 3.5 (t, J = 6.4 Hz, 2 H).

1-{2-[2-(1-(3,4-Dichlorophenyl)-1*H*-pyrazol-3-yloxy)ethoxy]-ethyl}piperidine (36). A mixture of **35** (0.17 g, 0.45 mmol), piperidine (0.062 g, 0.72 mmol), K_2CO_3 (0.25 g, 1.8 mmol), and NaI (0.067 g, 0.45 mmol) in DMF (5 mL) was stirred at 100 °C under a nitrogen atmosphere for 18 h. The solvent was evaporated in vacuo, and H_2O and diethyl ether were added. The aqueous phase was extracted with diethyl ether, and the combined organic phases were washed with H_2O, dried over Na_2SO_4, filtered, and evaporated to dryness in vacuo. The crude dark oil thus obtained was purified by column chromatography using mixtures of petroleum ether/EtOAc/MeOH of increasing polarity to give 1-{2-[2-(1-(3,4-dichlorophenyl)-1*H*-pyrazol-3-yloxy)ethoxy]-ethyl}piperidine as an oil (0.12 g, 69%): ^{1}H NMR (300 MHz, $CDCl_3$) δ 7.74 (d, J = 2.3 Hz, 1 H), 7.68 (d, J = 2.7 Hz, 1 H), 7.46 (d, J = 8.7 Hz, 1 H), 7.41 (dd, J = 8.8, 2.4 Hz, 1 H), 5.94 (d, J = 2.7 Hz, 1 H), 4.47−4.36 (m, 2 H), 3.91−3.78 (m, 4 H), 3.00−2.44 (m, 6 H), 1.89−1.60 (m, 4 H), 1.59−1.40 (m, 2 H).

2-[1-(3,4-Dichlorophenyl)-1*H*-pyrazol-3-yloxy]ethanol (37). A mixture of **8b** (0.24 g, 1.04 mmol), 2-bromoethanol (0.27 g, 2.08 mmol), K_2CO_3 (0.43 g, 3.12 mmol), and NaI (0.16 g, 1.04 mmol) in DMF (5 mL) was stirred at 60 °C under a nitrogen atmosphere for 18 h. The solvent was evaporated to dryness and the residue partitioned between H_2O and diethyl ether. The combined organic phases were washed with H_2O and dried over Na_2SO_4, filtered, and evaporated in vacuo. The residue was stirred with petroleum ether at 45 °C and decanted 3 times. The solid thus obtained was dried to give **37** (0.26 g, 91%) which was used without further purification in the next step: ^{1}H NMR ($CDCl_3$) δ 7.7 (d, J = 2.3 Hz, 1 H), 7.65 (d, J = 2.7 Hz, 1 H), 7.45 (d, J = 8.7 Hz, 1 H), 7.4 (dd, J = 2.3 and 8.7 Hz, 1 H), 5.95 (d, J = 2.7 Hz, 1 H), 4.4 (m, 2 H), 4.0 (m, 2 H).

2-[1-(3,4-Dichlorophenyl)-1*H*-pyrazol-3-yloxy]ethyl 2-Morpholinoethanesulfonate (40). To a solution of **37** (0.15 g, 0.53 mmol) and triethylamine (0.22 mL, 1.58 mmol) in CH_2Cl_2 (9 mL) was added a solution of **39** (prepared from 0.69 mmol of **38** and 0.14 mL, 1.57 mmol of oxalyl chloride in CH_2Cl_2 at 0 °C), and the final mixture was stirred at room temperature for 18 h. Water was added, and the organic phase was separated. The aqueous phase was extracted with more CH_2Cl_2, and the combined organic phases were washed with a saturated aqueous $NaHCO_3$ solution and dried over Na_2SO_4. The solvent was evaporated to give a residue, which was purified by column chromatography using petroleum ether/EtOAc, 8:2, as eluent. The solid thus obtained was crystallized from acetone−petroleum ether to give **40** as a white solid (0.094 g, 40%): mp 120−122 °C; ^{1}H NMR (DMSO-d_6) δ 8.49 (d, J = 2.7 Hz, 1 H), 8.03 (d, J = 2.3 Hz, 1 H), 7.76 (dd, J = 8.9, 2.3 Hz, 1 H), 7.72 (d, J = 8.9 Hz, 1 H), 6.15 (d, J = 2.7 Hz, 1 H), 4.62−4.52 (m, 2 H), 4.52−4.43 (m, 2 H), 3.59 (t, J = 7.3 Hz, 2 H), 3.53 (t, J = 4.7 Hz, 4 H), 2.69 (t, J = 7.3 Hz, 2 H), 2.39 (t, J = 4.6 Hz, 4 H).

1-[1-(3,4-Dichlorophenyl)-1*H*-pyrazol-3-yloxy]-3-morpholinopropan-2-ol (41a). A mixture of **8b** (0.20 g, 0.87 mmol), 2-(chloromethyl)oxirane (0.10 g, 1.05 mmol), K_2CO_3 (0.36 g, 2.62 mmol), and NaI (0.13 g, 0.87 mmol) in DMF (6 mL) was stirred at 100 °C for 4 h. The solvent was evaporated to dryness and the residue partitioned between H_2O and CH_2Cl_2. The combined organic phases were dried over Na_2SO_4, filtered, and evaporated in vacuo to yield 1-(3,4-dichlorophenyl)-3-(oxiran-2-ylmethoxy)-1*H*-pyrazole as a dark oil (0.24 g, 95%), which was used without further purification in next step. ^{1}H NMR ($CDCl_3$) δ 7.75 (d, J = 2.4 Hz, 1 H), 7.7 (d, J = 2.6 Hz, 1 H), 7.45 (d, J = 8.8 Hz, 1 H), 7.4 (dd, J = 2.5 and 8.8 Hz, 1 H), 5.95 (d, J = 2.6 Hz, 1 H), 4.55 (dd, J = 3.1 and 11.7 Hz, 1 H), 4.2 (dd, J = 6.0 and 11.7 Hz, 1 H), 3.4 (m, 1 H), 2.9 (dd, J = 5.0 and 9.1 Hz, 1 H), 2.75 (dd, J = 2.7 and 5.0 Hz, 1 H).

A mixture of the previous compound (0.23 g, 0.82 mmol), morpholine (0.072 g, 0.82 mmol), K_2CO_3 (0.34 g, 2.47 mmol), and NaI (0.123 g, 0.82 mmol) in DMF (6 mL) was heated to reflux for 8 h, after which the solvent was evaporated in vacuo. To the crude residue thus obtained were added H_2O and CH_2Cl_2. The aqueous solution was extracted several times with CH_2Cl_2, and the combined organic phases were washed with H_2O and dried over Na_2SO_4. The suspension was filtered and the solvent evaporated to dryness to give a crude compound, which was purified by column chromatography using mixtures of petroleum ether/EtOAc/MeOH of increasing polarity to give **41a** as an oil (0.114 g, 37%): ^{1}H NMR (300 MHz, $CDCl_3$) δ 7.72 (d, J = 2.5 Hz, 1 H), 7.70 (d, J = 2.7 Hz, 1 H), 7.47 (d, J = 8.8 Hz, 1 H), 7.41 (dd, J = 8.9,

2.5 Hz, 1 H), 5.95 (d, J = 2.7 Hz, 1 H), 4.49−4.25 (m, 3 H), 4.04−3.83 (m, 4 H), 3.11−2.74 (m, 6 H).

1-(3,4-Dichlorophenyl)-5-methyl-1*H*-pyrazole-3-thiol (42). A suspension of **8c** (R_1 = 3,4-dichlorophenyl, R_2 = Me, R_3 = H; obtained using method A; 8.00 g, 33 mmol) and P_2S_5 (7.33 g, 33 mmol) in xylenes (250 mL) was heated at reflux under a nitrogen atmosphere for 20 h. The mixture was cooled to room temperature. The precipitated solid was filtered off, and the filtrate was evaporated to dryness. The residue thus obtained was partitioned between toluene and 10% aqueous KOH solution, and the phases were separated. The combined organic phases were washed with H_2O, dried over Na_2SO_4, and concentrated to dryness to afford a yellow solid (2.20 g), which was identified as a mixture of **42** and 1,2-bis[1-(3,4-dichlorophenyl)-5-methyl-1*H*-pyrazol-3-yl]-disulfane. The aqueous phase was acidified with 2 N HCl solution and extracted again with EtOAc to obtain a mixture of the same two compounds (5.80 g). The two fractions (total 8.0 g) were suspended in EtOH (300 mL). $NaBH_4$ (11.13 g, 0.294 mol) was slowly added, and the reaction mixture was heated to reflux for 18 h. The solvent was evaporated under vacuum, and the residue was partitioned between CH_2Cl_2 and 2 N HCl aqueous solution. The combined organic phases were washed with H_2O, dried over Na_2SO_4, filtered, and evaporated to dryness to afford **42** as a brown oil (4.65 g, 55%): ^{1}H NMR (CD_3OD-d_4) δ 7.7 (m, 2 H), 7.45 (dd, J = 2.5 Hz, J' = 8.6 Hz, 1 H), 6.25 (s, 1 H), 2.3 (s, 3 H).

4-{2-[1-(3,4-Dichlorophenyl)-5-methyl-1*H*-pyrazol-3-ylthio]-ethyl}morpholine (43). A mixture of **42** (0.16 g, 0.63 mmol), 4-(2-chloroethyl)morpholine (0.13 g, 0.7 mmol), K_2CO_3 (0.26 g, 1.9 mmol), and a catalytic amount of NaI in dry DMF (6 mL) was stirred at 95 °C under a nitrogen atmosphere for 18 h. The solvent was evaporated and a mixture of H_2O/diethyl ether added to the crude residue. The organic extracts were washed with H_2O, dried over Na_2SO_4, and concentrated in vacuo to obtain **43** as an oil (0.17 g, 72%): ^{1}H NMR (300 MHz, $CDCl_3$) δ 7.59−7.54 (m, 2 H), 7.31 (dd, J = 8.8, 2.1 Hz, 1 H), 6.18 (s, 1 H), 4.04−3.92 (m, 4 H), 3.69−3.28 (m, 2 H), 3.67−3.54 (m, 2 H), 3.46−3.36 (m, 2 H), 3.36−3.25 (m, 2 H), 2.99−2.80 (m, 2 H), 2.33 (s, 3 H).

1-(3,4-Dichlorophenyl)-4,5-dihydro-1*H*-pyrazol-3-amine (44). A solution of NaOEt in EtOH was prepared by dissolving Na (0.40 g, 17.6 mmol) in EtOH (23 mL) under a nitrogen atmosphere. To this solution 3,4-dichlorophenylhydrazine hydrochloride, **5a** (1.85 g, 8 mmol), was added, and the mixture was heated to reflux for 45 min under vigorous stirring. The mixture was cooled to room temperature, and acrylonitrile (0.53 mL, 8 mmol) was added and the resulting solution heated again to reflux for 4 h. The red suspension was cooled and filtered, and the solid thus obtained was washed with EtOH, H_2O, and diethyl ether and dried under vacuum. Compound **44** was obtained as an off beige solid (1.10 g, 61% yield), which was used without further purification in the next step: ^{1}H NMR (DMSO-d_6) δ 7.25 (d, J = 8.9 Hz, 1 H), 6.85 (d, J = 2.6 Hz, 1 H), 6.65 (dd, J = 2.6 and 8.9 Hz, 1 H), 5.9 (s, 2 H), 3.5 (t, J = 9.2 Hz, 2 H), 2.8 (t, J = 9.4 Hz, 2 H).

1-(3,4-Dichlorophenyl)-1*H*-pyrazol-3-amine (45). To a solution of **44** (0.62 g, 2.7 mmol) in CH_2Cl_2 (45 mL) was added MnO_2 (1.04 g, 10.8 mmol), and the mixture was stirred at room temperature for 4 h. The resulting suspension was filtered through dicalite and the solvent evaporated to dryness in vacuo. A red crude solid was obtained, which was crystallized in ethyl ether/petroleum ether to give **45** (0.46 g, 74%). ^{1}H NMR (DMSO-d_6) δ 8.2 (d, J = 2.5 Hz, 1 H), 7.9 (bs, 1 H), 7.6 (m, 2 H), 5.75 (d, J = 2.5 Hz, 1 H), 5.2 (bs, 2 H).

***N*-[1-(3,4-Dichlorophenyl)-1*H*-pyrazol-3-yl]-2-morpholinoacetamide (46).** To a solution of **45** (0.36 g, 1.59 mmol) and triethylamine (0.24 g, 2.38 mmol) in dry THF (5 mL) was added 2-chloroacetyl chloride (0.20 g, 1.79 mmol) at 0 °C. The mixture was stirred for 18 h at room temperature. H_2O was added and the organic solvent evaporated in vacuo. The resulting suspension was filtered and dried to give 2-chloro-*N*-(1-(3,4-dichlorophenyl)-1*H*-pyrazol-3-yl)-acetamide as a beige solid (0.45 g, 93%): ^{1}H NMR ($CDCl_3$) δ 8.75 (br s, 1 H), 7.75 (d, J = 2.7 Hz, 1 H), 7.7 (d, J = 2.4 Hz, 1 H), 7.45 (d, J = 8.6 Hz, 1 H), 7.4 (dd, J = 2.4 and 8.6 Hz, 1 H), 6.9 (d, J = 2.7 Hz, 1 H), 4.15 (s, 2 H).

A mixture of the previous compound (0.22 g, 0.74 mmol), morpholine (0.071 g, 0.81 mmol), K_2CO_3 (0.22 g, 1.62 mmol), and NaI (0.11 g, 0.74 mmol) in dry DMF (5 mL) was heated to 100 °C under a nitrogen atmosphere for 18 h. The solvent was evaporated in vacuo, and H_2O was added to the crude residue. The dark solid thus precipitated was filtered and dried to give a crude product, which was purified by crystallization from EtOAc. Compound **46** was obtained as a beige solid (0.23 g, 87%): mp 125−127 °C; ^{1}H NMR ($CDCl_3$) δ 9.5 (br s, 1 H), 7.8 (2d, J = 2.8 and 2.4 Hz, 2 H), 7.5 (d, J = 8.5 Hz, 1 H), 7.45 (dd, J = 2.4 and 8.5 Hz, 1 H), 7.0 (d, J = 2.8 Hz, 1 H), 3.8 (m, 4 H), 3.2 (m, 2 H), 2.6 (m, 4 H).

1-(3,4-Dichlorophenyl)-*N*-(2-morpholinoethyl)-1*H*-pyrazol-3-amine (48). To an ice cooled solution of **46** (0.10 g, 0.28 mmol) in dry THF (4 mL), under a nitrogen atmosphere, a 2 M solution of BH_3·Me_2S in THF (0.7 mL, 1.4 mmol) was added dropwise. The solution was slowly warmed to reflux, kept at reflux temperature for 4 h, and stirred at room temperature for 16 h. After the mixture was cooled to 0 °C, H_2O (2 mL) and 6 M HCl (0.5 mL) were cautiously added and the mixture was heated to reflux for 2 h. Solvents were evaporated to dryness, and the residue was partitioned between 10% NaOH aqueous solution and EtOAc. The combined organic phases were washed with H_2O, dried over Na_2SO_4, filtered, and evaporated to dryness. The crude residue was purified by column chromatography using mixtures of petroleum ether/EtOAc of increasing polarity as eluent to give **48** as an oil (0.053 g, 56%): ^{1}H NMR (300 MHz, $CDCl_3$) δ 7.72 (d, J = 2.4 Hz, 1 H), 7.66 (d, J = 2.7 Hz, 1 H), 7.43 (d, J = 8.7 Hz, 1 H), 7.38 (dd, J = 8.8, 2.4 Hz, 1 H), 5.87 (d, J = 2.7 Hz, 1 H), 3.97−3.68 (m, 4 H), 3.54−3.29 (m, 2 H), 3.02−2.39 (m, 6 H).

4-[2-(5-Methyl-1*H*-pyrazol-3-yloxy)ethyl]morpholine (51). To a suspension of **50** (21.5 g, 0.22 mol) in CH_2Cl_2 (150 mL), a solution of $(Boc)_2O$ (47.80 g, 0.22 mol) and triethylamine (32 mL, 0.23 mol) in CH_2Cl_2 (50 mL) was added. The mixture was stirred at room temperature for 18 h, after which the organic solvent was evaporated in vacuo. The resulting crude product was recrystallized from toluene to give *tert*-butyl 3-hydroxy-5-methyl-1*H*-pyrazole-1-carboxylate as a white solid (32.60 g, 75%): ^{1}H NMR (400 MHz, DMSO-d_6) δ 10.69 (sb, 1 H), 5.70 (d, J = 1.1 Hz, 1 H), 2.37 (d, J = 1.0 Hz, 3 H), 1.52 (s, 9 H).

To a solution of the previous compound (18.30 g, 0.092 mol) in DMF (200 mL) were added KI (0.69 g, 0.005 mol), K_2CO_3 (38.28 g, 0.277 mol), and 4-(2-chloroethyl)morpholine hydrochloride (16.32 g, 0.088 mol). The reaction mixture was heated at 95 °C for 20 h and then allowed to reach room temperature. The solvent was removed in vacuo, and the crude residue was taken up in a mixture of H_2O and diethyl ether. The organic layers were dried over Na_2SO_4 and evaporated to dryness to give *tert*-butyl 5-methyl-3-(2-morpholinoethoxy)-1*H*-pyrazole-1-carboxylate as a red solid (19.97 g, 72%), which was used without further purification in the next step: ^{1}H NMR (300 MHz, DMSO-d_6) δ 5.90 (s, 1 H), 4.21 (t, J = 5.7 Hz, 2 H), 3.63−3.49 (m, 4 H), 2.64 (t, J = 5.6 Hz, 2 H), 2.47−2.40 (m, 4 H), 2.38 (s, 3 H), 1.54 (s, 9 H).

To an ice-cooled solution of the previous compound (19.97 g, 0.064 mol) in EtOH (380 mL) was added 150 mL of aqueous 3 N HCl solution, and the mixture was allowed to reach room temperature and stirred for 1 h. The solvent was removed under reduced pressure to give 4-[2-(5-methyl-1*H*-pyrazol-3-yloxy)ethyl]morpholine hydrochloride as a yellow solid (19.70 g).

A solution of the previous compound (3.00 g, 12.11 mmol) in H_2O was basified with 10% NaOH solution. EtOAc was added, and the phases were separated. The combined organic fractions were dried over Na_2SO_4, and the solvent was removed under reduced pressure. The residue was dried under vacuum to give **51** as an orange oil (1.30 g, 50%), which was used without further purification in the next step: ^{1}H NMR (300 MHz, CD_3OD) δ 6.02 (s, 1 H), 4.70−4.60 (m, 2 H), 4.16−3.77 (m, 6 H), 3.72−3.62 (m, 2 H), 3.65−3.37 (m, 2 H), 2.36 (s, 3 H).

4-{2-[3-Methyl-1-(naphthalen-2-yl)-1*H*-pyrazol-5-yloxy]-ethyl}morpholine (52). To a solution of **51** (0.185 g, 0.88 mmol) in CH_2Cl_2 (10 mL) were added 2-naphthaleneboronic acid (0.165 g, 0.96 mmol), pyridine (141 μL, 1.75 mmol), $Cu(OAc)_2$·H_2O (0.26 g, 1.31 mmol), and 4 Å molecular sieves (1.0 g). The mixture was stirred at room temperature for 18 h in air and then evaporated. The residue thus obtained was purified by flash chromatography (cyclohexane/EtOAc) to provide **52** (0.088 g, 30%): ^{1}H NMR (400 MHz, $CDCl_3$) δ 8.14 (d, J = 2.0 Hz, 1 H), 7.93 (dd, J = 8.9, 2.1 Hz, 1 H), 7.90−7.79 (m, 3 H),

dx.doi.org/10.1021/jm3007323 | J. Med. Chem. 2012, 55, 8211−8224

7.53−7.41 (m, 2 H), 5.55 (s, 1 H), 4.25 (t, J = 5.6 Hz, 2 H), 3.78−3.64 (m, 4 H), 2.83 (t, J = 5.6 Hz, 2 H), 2.62−2.48 (m, 4 H), 2.32 (s, 3 H). The regioisomer **28** was also isolated (0.044 g, 15%).

Human σ_1 Receptor Radioligand Assay.[28] The binding properties of the test compounds to human σ_1R were studied in transfected HEK-293 membranes using [^{3}H](+)-pentazocine (Perkin-Elmer, NET-1056) as the radioligand. The assay was carried out with 7 μg of membrane suspension, [^{3}H](+)-pentazocine (5 nM) in either the absence or presence of either buffer or 10 μM haloperidol for total and nonspecific binding, respectively. Binding buffer contained Tris-HCl (50 mM, at pH 8). Plates were incubated at 37 °C for 120 min. After the incubation period, the reaction mix was transferred to MultiScreen HTS FC plates (Millipore), filtered, and plates were washed (3 times) with ice-cold Tris-HCl (10 mM, pH 7.4). Filters were dried and counted at approximately 40% efficiency in a MicroBeta scintillation counter (Perkin-Elmer) using EcoScint liquid scintillation cocktail.

Guinea Pig σ_2 Receptor Radioligand Assay. The binding properties of test compounds to guinea pig σ_2R were studied in guinea pig brain membranes as described[29] with some modifications. [^{3}H]Di-*o*-tolylguanidine (DTG) (Perkin-Elmer, code NET-986) was used as the radioligand. The assay was carried out with 200 μg of membrane suspension, [^{3}H]DTG (10 nM) in either absence or presence of either buffer or 10 μM haloperidol for total and nonspecific binding, respectively. Binding buffer contained Tris-HCl (50 mM, pH 8), and σ_1 receptor was blocked with (+)-SKF10047 at 400 nM. Plates were incubated at 25 °C for 120 min. After the incubation period, the reaction mix was transferred to MultiScreen HTS, FC plates (Millipore), filtered and plates were washed 3 times with ice-cold 50 mM Tris-HCl (pH 7.4). Filters were dried and counted at approximately 40% efficiency in a MicroBeta scintillation counter (Perkin-Elmer) using EcoScint liquid scintillation cocktail.

In Vitro Metabolic Stability in Human Liver Microsomes. The assay was carried out in a robotic liquid handling system (Packard Multiprobe II, Perkin-Elmer). All incubations were performed individually for each test compound. Compounds (10 μM) were incubated in 96-well plates at 37 °C during 1 h under standard incubation conditions: sodium−potassium phosphate buffer (50 mM, pH 7.4), $MgCl_2$ (3 mM), the NADPH-regenerating system, and CYP content (0.3 nmol/mL). At preset times (0, 10, 20, 40, and 60 min) aliquots of the reaction mixture were stopped with an equal volume of cold acetonitrile. Upon centrifugation of the resultant mixture, supernatants were analyzed by a generic UPLC−MS/MS method. Metabolic stability was determined by the disappearance of compound over time.[31,41] The ln-linear plots of the % of compound remaining based on chromatographic peak area versus time were plotted, and the slope was calculated by linear fitting of the curve. The in vitro metabolic half-life ($t_{1/2}$) was estimated by using $0.693/k$ where k is the biotransformation rate constant and corresponds to the slope of the ln-linear curve. The microsomal intrinsic clearance (Cl_{int}) was calculated using the equation $Cl_{int} = 0.693/[(t_{1/2})(\text{mg of microsomal protein/volume of incubation})]$.

In Vivo Tests. Animals. CD1 mice (Charles River, France) aged from 6 to 8 weeks old were used. Male mice were used for neuropathic pain studies and female mice for the capsaicin test. Animals had access to food and water ad libitum and were kept in controlled laboratory conditions with temperature at 21 ± 1 °C and a light−dark cycle of 12 h (lights on at 7:00 a.m.). Experimental behavioral testing was carried out in a soundproof and air-regulated experimental room and was done blind with respect to treatment and surgical procedure. Experimental procedures and animal husbandry were conducted according to European guidelines regarding protection of animals used for experimental and other scientific purposes (Council Directive of November 24, 1986, 86/609/ECC) and received approval by the local ethical committee.

Capsaicin Test. Capsaicin (8-methyl-*N*-vanillyl-6-nonamide) was purchased from Sigma-Aldrich and dissolved in 1% DMSO (vehicle) in physiological saline. Test compounds were dissolved in 0.5% hydroxypropylmethylcellulose (HPMC) (Sigma-Aldrich) and were administered in a volume of 10 mL/kg through the ip route. Mice were habituated for 2 h in individual test compartments placed on an elevated mesh bottomed platform with a 0.5 cm^2 grid to provide access to the ventral side of the paws and were then given an ipl injection of capsaicin (1 μg in 20 μL of 1% DMSO) into the mid-plantar surface of the right hind paw. Fifteen minutes after ipl capsaicin, mechanical stimulation was applied onto the plantar surface of the hind paw using an automated testing device (dynamic plantar aesthesiometer; Ugo Basile, Italy). The device lifts a straight monofilament (0.5 mm in diameter) exerting a constant upward pressure of 0.5 g (4.90 mN) onto the plantar surface, and when the animal withdraw its hind paw, the mechanical stimulus automatically stops and the latency time is recorded. Latency was defined as the time from the onset of exposure to the filament to the cessation of the pressure when the sensor detected the paw withdrawal. Paw withdrawal latencies were measured in triplicate for each animal at 30 s intervals. A cutoff latency of 60 s was used in each trial. Mice (n = 8−12 per group) received vehicle or drug through the ip route 15 min before capsaicin injection, and withdrawal latencies to mechanical stimulation were determined 15 min after capsaicin injection (30 min after treatments). The effect of treatments on mechanical hypersensitivity induced by capsaicin was calculated with the following equation: % reduction of mechanical hypersensitivity = $[(\text{LTD} - \text{LTV})/(\text{CT} - \text{LTV})] \times 100$, where LTD and LTV are the latency time in drug- and vehicle-treated animals, respectively, and CT is the cutoff time (60 s).

Partial Sciatic Nerve Ligation Model. The partial sciatic nerve ligation model was used to study the efficacy of treatments in neuropathic pain. Briefly, mice were anesthetized with isoflurane (Abbott-Esteve) (induction, 3%; surgery, 1%) and the common sciatic nerve was exposed at the level of the mid-thigh of the right hind paw. At about 1 cm proximal to the nerve trifurcation, a tight ligation using 9−0 nonabsorbable virgin silk suture (Alcon Surgical, U.S.) was created enclosing the outer 33−50% of the diameter of the sciatic nerve. The muscle was then stitched with 6−0 silk suture and the skin incision closed with wound clips. Two tests were performed: von Frey test first (30 min after treatment) and plantar test second (45 min after treatment). At 1 day after baseline measurements, sciatic nerve injury was induced and mice were tested after the surgical procedure to monitor the development of neuropathic-pain-related behaviors. On day 10 these behaviors were already apparent and mice received a vehicle injection. On days 11, 12, and 13, mice received ip administration of the drugs following a Latin square design (n = 10−12 per group). Allodynia to mechanical stimuli and hyperalgesia to noxious thermal stimulus were used as outcome measures of neuropathic pain by using the von Frey and plantar test, respectively. Briefly, in the von Frey test, animals were placed into compartment enclosures in a test chamber with a framed metal mesh floor through which the von Frey monofilaments (bending force range from 0.008 to 2.0 g) (North Coast Medical, Inc., U.S.) were applied and thresholds were measured in the ipsilateral, nerve-injured paw using the up−down paradigm. Clear paw withdrawal, shaking, or licking was considered as a nociceptive-like response. The effect of treatments on mechanical hypersensitivity induced by the operation was calculated with the following equation: % reduction of mechanical hypersensitivity = $[(\text{TRD} - \text{TRV})/(B - \text{TRV})] \times 100$, where TRD and TRV are the threshold pressure responses in drug- and vehicle-treated animals, respectively, and B is the basal pressure response (before operation). Thermal (heat) hyperalgesia was assessed with a plantar test apparatus (Ugo Basile), by measuring hind paw withdrawal latency in response to radiant heat. Briefly, mice were placed into compartment enclosures on a glass surface. The heat source was then positioned under the plantar surface of the hind paw and activated with a light beam intensity chosen based on preliminary studies to give baseline latencies from 8 to 9 s in control mice. The digital timer connected to the heat source automatically recorded the response latency for paw withdrawal to the nearest 0.1 s. A cutoff time of 20 s was imposed to prevent tissue damage in the absence of response. The mean withdrawal latencies for the ipsilateral hind paw were determined from the average of three separate trials done at 5 min intervals. The effect of treatments on thermal (heat) hypersensitivity induced by the operation was calculated with the following equation: % reduction of thermal hypersensitivity = $[(\text{LTD} - \text{LTV})/(B - \text{LTV})] \times 100$, where LTD and LTV are the

latency times in drug- and vehicle-treated animals, respectively, and *B* is the basal latency time.

Motor Coordination (Rotarod Test). The motor performance of mice was assessed by means of an automated rotarod (Panlab SL, Spain). Before drug treatments, mice were trained and those that were unable to stay moving on the rod for 240 s at 10 rpm were discarded for the study. Mice were required to walk against the motion of an elevated rotating drum at 10 rpm, and the latency to fall-down was recorded automatically. With the selected animals rotarod latencies were measured 30, 60, 120, and 180 min after ip administration of drugs.

■ ASSOCIATED CONTENT

Supporting Information

Analytical and characterization data for all the compounds and description of methods used for drug transport assay using Caco-2 cells, CYP inhibition, and pharmacokinetic studies of compound **28**. This material is available free of charge via the Internet at http://pubs.acs.org.

■ AUTHOR INFORMATION

Corresponding Author

*Phone: 0034934466000. E-mail: jldiaz@esteve.es.

Notes

The authors declare no competing financial interest.

■ ACKNOWLEDGMENTS

We thank Magda Bordas, Carme Calvet, and Raquel Enrech for their expert contribution to the analysis of the compounds; Albert Dordal, Xavier Monroy, Xavier Codony, Inés Álvarez, Eva Ayet, and Ariadna Balada for their expert contribution to ADME and in vivo studies; Miguel Angel Blázquez, Mónica Carro, Joan Andreu Morató, and Edmundo Ortega for their excellent technical assistance; and Carlos Pérez, Oscar Ferré, and Eduardo Villarroel for their contributions to compound management.

■ ABBREVIATIONS USED

S1RA, E-52862, 4-{2-[5-methyl-1-(naphthalen-2-yl)-1*H*-pyrazol-3-yloxy]ethyl}morpholine; ADME, absorption, distribution, metabolism, and excretion; CFA, Freund's complete adjuvant; TNBS, 2,4,6-trinitrobenzenesulfonic acid

■ REFERENCES

(1) Quirion, R.; Bowen, W. D.; Itzhak, Y.; Junien, J. L.; Musacchio, J. M.; Rothman, R. B.; Su, T. P.; Tam, S. W.; Taylor, D. P. A proposal for the classification of sigma binding sites. *Trends Pharmacol. Sci.* **1992**, *13*, 85−86.

(2) (a) Hanner, M.; Moebius, F. F.; Flandorfer, A.; Knaus, H. G.; Striessnig, J.; Kempner, E.; Glossmann, H. Purification, molecular cloning, and expression of the mammalian $sigma_1$-binding site. *Proc. Natl. Acad. Sci. U.S.A.* **1996**, *93*, 8072−8077. (b) Kekuda, R.; Prasad, P. D.; Fei, Y. J.; Leibach, F. H.; Ganapathy, V. Cloning and functional expression of the human type 1 sigma receptor (hSigmaR1). *Biochem. Biophys. Res. Commun.* **1996**, *229*, 553−558.

(3) Su, T. P.; Hayashi, T.; Maurice, T.; Buch, S.; Ruoho, A. E. The sigma-1 receptor chaperone as an inter-organelle signalling modulator. *Trends Pharmacol. Sci.* **2010**, *31*, 557−566.

(4) Monnet, F. P.; Debonnel, G.; Junien, J. L.; De Montigny, C. *N*-Methyl-D-aspartate-induced neuronal activation is selectively modulated by sigma receptors. *Eur. J. Pharmacol.* **1990**, *179*, 441−445.

(5) Cheng, Z. X.; Lan, D. M.; Wu, P. Y.; Zhu, Y. H.; Dong, Y.; Ma, L.; Zheng, P. Neurosteroid dehydroepiandrosterone sulphate inhibits persistent sodium currents in rat medial prefrontal cortex via activation of sigma-1 receptors. *Exp. Neurol.* **2010**, *210*, 128−136.

(6) Chien, C. C.; Pasternak, G. W. Selective antagonism of opioid analgesia by a sigma system. *J. Pharmacol. Exp. Ther.* **1994**, *271*, 1583−1590.

(7) Kim, F. J.; Kovalyshyn, I.; Burgman, M.; Neilan, C.; Chien, C. C.; Pasternak, G. W. Sigma-1 receptor modulation of G-protein-coupled receptor signaling: potentiation of opioid transduction independent from receptor binding. *Mol. Pharmacol.* **2010**, *77*, 695−703.

(8) (a) Zamanillo, D.; Portillo-Salido, E; Vela, J. M.; Romero, L. Sigma 1 Receptor Chaperone: Pharmacology and Therapeutic Perspectives. In *Therapeutic Targets*; Botana, J. M., Loza, M.; Eds.; John Wiley & Sons: Hoboken, NJ, 2012; Chapter 6, pp 225−278. (b) Maurice, T.; Su, T. P. The pharmacology of sigma-1 receptors. *Pharmacol. Ther.* **2009**, *124*, 195−206.

(9) Marrazzo, A.; Cobos, E. J.; Parenti, C.; Arico, G.; Marrazzo, G.; Ronsisvalle, S.; Pasquinucci, L.; Prezzavento, O.; Colabufo, N. A.; Contino, M. A.; Gonzalez, L. G.; Scoto, M. G.; Ronsisvalle, G. Novel potent and selective sigma ligands: evaluations of their agonist and antagonist properties. *J. Med. Chem.* **2011**, *54*, 3669−3673.

(10) Crawford, K. W.; Bowen, W. D. Sigma-2 receptor agonists activate a novel apoptotic pathway and potentiate antineoplastic drugs in breast tumor cell lines. *Cancer Res.* **2002**, *1*, 313−322.

(11) Cendán, C. M.; Pujalte, J. M.; Portillo-Salido, E.; Montoliu, L.; Baeyens, J. M. Formalin-induced pain is reduced in sigma(1) receptor knockout mice. *Eur. J. Pharmacol.* **2005**, *511*, 73−74.

(12) Entrena, J. M.; Cobos, E. J.; Nieto, F. R.; Cendán, C. M.; Gris, G.; Del Pozo, E.; Zamanillo, D.; Baeyens, J. M. Sigma-1 receptors are essential for capsaicin-induced mechanical hypersensitivity: studies with selective sigma-1 ligands and sigma-1 knockout mice. *Pain* **2009**, *143*, 252−261.

(13) De la Puente, B.; Nadal, X.; Portillo-Salido, E.; Sánchez-Arroyos, R.; Ovalle, S.; Palacios, G.; Muro, A.; Romero, L.; Entrena, J. M.; Baeyens, J. M; López-García, J. A.; Maldonado, R.; Zamanillo, D.; Vela, J. M. Sigma-1 receptors regulate activity-induced spinal sensitization and neuropathic pain after peripheral nerve injury. *Pain* **2009**, *145*, 294−303.

(14) Cendán, C. M.; Pujalte, J. M.; Portillo-Salido, E.; Baeyens, J. M. Antinociceptive effects of haloperidol and its metabolites in the formalin test in mice. *Psychopharmacology (Berlin)* **2005**, *182*, 485−493.

(15) Roh, D. H.; Kim, H. W.; Yoon, S. Y.; Seo, H. S.; Kwon, Y. B.; Kim, K. W.; Han, H. J.; Beitz, A. J.; Na, H. S.; Lee, J. H. Intrathecal injection of the sigma 1 receptor antagonist BD1047 blocks both mechanical allodynia and increases in spinal NR1 expression during the induction phase of rodent neuropathic pain. *Anesthesiology* **2008**, *109*, 879−889.

(16) Drews, E.; Zimmer, A. Central sensitization needs sigma receptors. *Pain* **2009**, *145*, 269−270.

(17) Díaz, J. L.; Zamanillo, D.; Corbera, J.; Baeyens, J. M.; Maldonado, R.; Pericàs, M. A.; Vela, J. M.; Torrens, A. Selective sigma-1 receptor antagonists: emerging target for the treatment of neuropathic pain. *Cent. Nerv. Syst. Agents Med. Chem.* **2009**, *9*, 172−183.

(18) Romero, L.; Zamanillo, D.; Nadal, X.; Sánchez-Arroyos, R.; Rivera-Arconada, I.; Dordal, A.; Montero, A.; Muro, A.; Bura, A.; Segalés, C.; Laloya, M.; Hernández, E.; Portillo-Salido, E.; Escriche, M.; Codony, X.; Encina, G.; Burgueño, J.; Merlos, M.; Baeyens, J. M.; Giraldo, J.; López-García, J. A.; Maldonado, R.; Plata-Salamán, C. R.; Vela, J. M. Pharmacological properties of S1RA, a new sigma-1 receptor antagonist that inhibits neuropathic pain and activity-induced spinal sensitization. *Br. J. Pharmacol.* [Online early access]. DOI: 10.1111/j.1476-5381.2012.01942.x. Published Online: Mar 9, **2012**.

(19) Abadias, M.; Escriche, M.; Vaqué, A.; Sust, M.; Encina, G. Safety, tolerability and pharmacokinetics of single and multiple doses of a novel sigma-1 receptor antagonist in three randomized phase I studies. *Br. J. Clin. Pharmacol.* [Online early access]. DOI: 10.1111/j.1365-2125.2012.04333.x. Published Online: May 21, **2012**.

(20) (a) Laggner, C.; Cuberes, R.; Holenz, J.; Berrocal, J.; Contijoch, M. PCT Pat. Appl. WO2006/021462, 2006. (b) Cuberes, R.; Holenz, J. PCT Pat. Appl. WO2007/098963, 2007. (c) Cuberes, R.; Holenz, J. PCT Pat. Appl. WO2007/098964, 2007. (d) Cuberes, R.; Holenz, J. PCT Pat. Appl. WO2007/098967, 2007.

(21) Gaede, B. J.; McDermott, L. L. Novel perfluoroalkyl-substituted pyrazoles. 1. Hydroxypyrazoles. *J. Heterocycl. Chem.* **1993**, *30*, 49−54.

(22) Koenig, H.; Goetz, N.; Kirstgen, R.; Mueller, B.; Oberdorf, K. Eur. Pat. Appl. EP680954, 1995.
(23) Doria, G.; Passarotti, C.; Sala, R.; Magrini, R.; Sberze, P.; Tibolla, M.; Ceserani, R.; Castello, R. Synthesis and antiulcer activity of (*E*)-5-[2-(3-pyridyl)ethenyl]-1*H*,7*H*-pyrazolo[1,5-*a*]pyrimidine-7-ones. *Farmaco* **1986**, *41*, 417−429.
(24) Rossiter, S.; Woo, C. K.; Hartzoulakis, B.; Wishart, G.; Stanyer, L.; Labadie, J. W.; Selwood, D. L. Copper(II)-mediated arylation with aryl boronic acids for the N-derivatization of pyrazole libraries. *J. Comb. Chem.* **2004**, *6*, 385−390.
(25) Rack, E.; Fröhlich, R.; Schepmann, D.; Wünsch, B. Design, synthesis and pharmacological evaluation of spirocyclic σ_1 receptor ligands with exocyclic amino moiety (increased distance 1). *Bioorg. Med. Chem.* **2011**, *19*, 3141−3151.
(26) Glennon, R. A.; Ablordeppey, S. A.; Ismaiel, A. M.; El-Ashmawy, M. B.; Fischer, J. B.; Howie, K. B. Structural features important for σ_1 receptor binding. *J. Med. Chem.* **1994**, *37*, 1214−1219.
(27) Laggner, C.; Schieferer, C.; Fiechtner, B.; Poles, G.; Hoffmann, R. D.; Glossmann, H.; Langer, T.; Moebius, E. F. Discovery of high-affinity ligands of σ1 receptor, ERG2, and emopamil binding protein by pharmacophore modeling and virtual screening. *J. Med. Chem.* **2005**, *48*, 4754−4764.
(28) DeHaven-Hudkins, D. L.; Fleissner, L. C.; Ford-Rice, F. Y. Characterization of the binding of [^{3}H](+)pentazocine to recognition sites in guinea pig brain. *Eur. J. Pharmacol.* **1992**, *227*, 371−378.
(29) Ronsisvalle, G.; Marrazzo, A.; Prezzavento, O.; Cagnotto, A.; Mennini, T.; Parenti, C.; Scoto, G. M. Opioid and sigma receptor studies. New developments in the design of selective sigma ligands. *Pur. Appl. Chem.* **2001**, *73*, 1499−1509.
(30) Costa, B. R.; Radesca, L.; di Paolo, L.; Bowen, W. D. Synthesis, characterization, and biological evaluation of a novel class of *N*-(arylethyl)-*N*-alkyl-2-(1-pyrrolidinyl)ethylamines: structural requirements and binding affinity at the sigma receptor. *J. Med. Chem.* **1992**, *35*, 38−47.
(31) (a) Obach, R. S.; Baxter, J. G.; Liston, T. E.; Silber, B. M.; Jones, B. C.; MacIntyre, F.; Rance, D. J.; Wastall, P. The prediction of human pharmacokinetic parameters from preclinical and in vitro metabolism data. *J. Pharmacol. Exp. Ther.* **1997**, *283*, 46−58. (b) Obach, R. S. Prediction of human clearance of twenty-nine drugs from hepatic microsomal intrinsic clearance data: an examination of in vitro half-life approach and nonspecific binding to microsomes. *Am. Soc. Pharmacol. Exp. Ther.* **1999**, *27*, 1350−1359.
(32) Diaz, G. J.; Daniell, K.; Leitza, S. T.; Martin, R. L.; Su, Z.; McDermott, J. S.; Cox, B. F.; Gintant, G. A. The [^{3}H]-dofetilide binding assay is a predictive screening tool for hERG blockade and proarrhythmia: comparison of intact cell and membrane preparations and effects of altering $[K^+]_o$. *J. Pharmacol. Toxicol. Methods* **2004**, *50*, 187−199.
(33) Cobos, E. J.; Baeyens, J. M.; Del Pozo, E. Phenytoin differentially modulates the affinity of agonist and antagonist ligands for sigma 1 receptors of guinea pig brain. *Synapse* **2005**, *55*, 192−195.
(34) Vidal-Torres, A.; Touriño, C.; Romero, L.; Baeyens, J. M.; Zamanillo, D.; Maldonado, R.; Vela, J. M. Potentiation of morphine analgesia but inhibition of the rewarding effects of morphine following co-administration of a new selective sigma-1 receptor antagonist. *Eur. J. Pain* **2009**, *3* (Suppl. 1), Abstract 341, S104.
(35) Gris, G.; Vidal, A.; Fort, M.; Aubel, B.; Romero, L.; González, A.; Portillo-Salido, E.; Baeyens, J. M.; Vela, J. M.; Deseure, K.; Zamanillo, D. Analgesic efficacy in rat models of experimental pain of a new selective sigma-1 receptor antagonist. *Eur. J. Pain* **2009**, *3* (Suppl. 1), Abstract 335, S102.
(36) Malmberg, A. B.; Basbaum, A. I. Partial sciatic nerve injury in the mouse as a model of neuropathic pain: behavioral and neuroanatomical correlates. *Pain* **1998**, *76*, 215−222.
(37) Wager, T. T.; Hou, X.; Verhoest, P. R.; Villalobos, A. Moving beyond rules: the development of a central nervous system multiparameter optimization (CNS MPO) approach to enable alignment of druglike properties. *ACS Chem. Neurosci.* **2010**, *1*, 435−449.
(38) Hu, M.; Ling, J.; Lin, H.; Chen, J. Use of Caco-2 Cell Monolayers To Study Drug Absorption and Metabolism. In *Optimization in Drug Discovery: In Vitro Methods*; Yan, Z., Caldwell, G. W., Eds.; Humana Press, Totowa, NJ, 2004; pp 19−36.
(39) (a) Stresser, D. M. High-Throughput Screening of Human Cytochrome P450 Inhibitors Using Fluorometric Substrates. Methodology for 25 Enzyme/Substrate Pairs. In *Optimization in Drug Discovery: In Vitro Methods*; Yan, Z., Caldwell, G. W., Eds.; Humana Press: Totowa, NJ, 2004; pp 215−230. (b) Yan, Z.; Caldwell G. W. Evaluation of Cytochrome P450 Inhibition in Human Liver Microsomes. In *Optimization in Drug Discovery: In Vitro Methods*; Yan, Z., Caldwell, G. W., Eds.; Humana Press: Totowa, NJ, 2004; pp 231−244; (c) Drug Interaction Studies—Study Design, Data Analysis, Implications for Dosing and Labeling. U.S. Department of Health and Human Services, Food and Drug Administration, Center for Drug Evaluation and Research (CDER), September 2006 and February 2012.
(40) Box, K. J.; Comer, E. A. Using measured pKa, logP and solubility to investigate supersaturation and predict BCS class. *Curr. Drug Metab.* **2008**, *9*, 869−878.
(41) (a) Di, L.; Kerns, E. H.; Hong, Y.; Kleintop, T. A.; McConnell, O. J.; Huryn, D. M. Optimization of a higher throughput microsomal stability screening assay for profiling drug discovery candidates. *J. Biomol. Screening* **2003**, *8*, 453−462. (b) Di, L.; Kerns, E. H.; Gao, N.; Li, S. Q.; Huang, Y.; Bourassa, J. L.; Huryn, D. M. Experimental design of single-time-point high-throughput microsomal stability assay. *J. Pharmacol. Sci.* **2004**, *93*, 1537−1544.